

1 **Neuraminidase inhibitors rewire neutrophil function in murine sepsis and COVID-**
2 **19 patient cells**

3
4 Rodrigo O. Formiga^{1,2}, Flávia C. Amaral^{1,2}, Camila F. Souza², Daniel A. G. B.
5 Mendes^{1,2}, Carlos W. S. Wanderley³, Cristina B. Lorenzini^{1,2}, Adara A. Santos^{1,4},
6 Juliana Antônia¹, Lucas F. Faria¹, Caio C. Natale^{1,2}, Nicholas M. Paula^{1,2}, Priscila C. S.
7 Silva¹, Fernanda R. Fonseca⁵, Luan Aires^{1,2}, Nicoli Heck¹, Shana P. C. Barroso⁶,
8 Alexandre Morrot⁷, Regina Sordi², Frederico Alisson-Silva⁸, Daniel S. Mansur^{1,4},
9 Fernando Q. Cunha³, Rosemeri Maurici⁵, André Báfica^{1,4}, Matthew S. Macauley^{9,10},
10 Fernando Spiller^{1,2*}

11
12 ¹Laboratory of Immunobiology, ²Department of Pharmacology, ⁴Department of
13 Microbiology, Immunology and Parasitology, ⁵Department of Clinical Medicine, Federal
14 University of Santa Catarina (UFSC), Florianópolis, Santa Catarina, Brazil.

15 ³Department of Pharmacology, School of Medicine of Ribeirao Preto, University of Sao
16 Paulo, Ribeirao Preto, Sao Paulo, Brazil.

17 ⁶Molecular Biology Laboratory, Institute of Biomedical Research, Marcilio Dias Naval
18 Hospital, Navy of Brazil, Rio de Janeiro, Brazil.

19 ⁷Tuberculosis Research Laboratory, Faculty of Medicine, Federal University of Rio de
20 Janeiro, Rio de Janeiro, Brazil; Immunoparasitology Laboratory, Oswaldo Cruz
21 Foundation, FIOCRUZ, Rio de Janeiro, Brazil.

22 ⁸Department of Immunology, Paulo de Goes Institute of Microbiology, Federal University
23 of Rio de Janeiro (UFRJ), Rio de Janeiro, Brazil.

24 ⁹Department of Chemistry, ¹⁰Department of Medical Microbiology and Immunology,
25 University of Alberta, Edmonton, Alberta, Canada.

26
27 *Corresponding author: Fernando Spiller, Department of Pharmacology
28 (FMC/CCB/UFSC), Av. Prof. Henrique da Silva Fontes, 321 - Trindade, Florianópolis –
29 SC, 88040-900, Tel.: +55-48-3721-4852. e-mail: fernando.spiller@ufsc.br,
30 spiller.farmaco@gmail.com.

31

32 **ABSTRACT**

33

34 Neutrophils overstimulation plays a crucial role in tissue damage during severe
35 infections. Neuraminidase-mediated cleavage of surface sialic acid has been
36 demonstrated to regulate leukocyte responses. Here, we report that antiviral
37 neuraminidase inhibitors constrain host neuraminidase activity, surface sialic acid
38 release, ROS production, and NETs released by microbial-activated human neutrophils.
39 *In vivo*, treatment with Oseltamivir results in infection control and host survival in murine
40 models of sepsis. Moreover, Oseltamivir or Zanamivir treatment of whole blood cells
41 from severe COVID-19 patients reduces host NEU-mediated shedding of surface sialic
42 acid and neutrophil overactivation. These findings suggest that neuraminidase inhibitors
43 are host-directed interventions to dampen neutrophil dysfunction in severe infections.

44

45 Keywords: neuraminidase; sialic acid; sepsis; Oseltamivir; Zanamivir, neutrophil; SARS-
46 CoV-2; COVID-19.

47

48

49 INTRODUCTION

50

51 Neutrophils are key components of the immune response against multiple pathogens¹.
52 However, during acute severe infections, such as sepsis and COVID-19, overactivated
53 neutrophils infiltrate vital organs and release many molecules including proteases,
54 reactive oxygen species (ROS), and neutrophil extracellular traps (NETs)^{2,3}. While such
55 inflammatory mediators are essential to the control of infection, they can also damage
56 healthy cells⁴. Therefore, the function of neutrophils must be regulated to efficiently
57 clear microorganisms with minimal detrimental effects to the host.

58

59 A number of mechanisms controlling neutrophil activation have been described⁵. For
60 instance, the contents of sialic acid (Sia) have been demonstrated to regulate leukocyte
61 activation to microbial stimuli^{6,7}. The dense array of Sia present in the glycocalyx of all
62 mammalian cells makes this monosaccharide a central molecule for many cellular
63 processes including: cell-cell interaction, signal transduction, and transendothelial
64 migration⁸. Neuraminidases (NEUs) are enzymes found in both pathogens and
65 mammalian hosts⁹, which hydrolyze Sia residues linked to galactose, N-
66 acetylgalactosamine or polySia residues on glycoconjugates, thereby regulating many
67 physiological and pathological responses¹⁰. In human neutrophils, shedding of surface
68 Sia by microbial-derived NEUs leads to cellular activation, ROS production, and NETs
69 release^{7,11-13}. Additionally, it has been demonstrated that LPS induces membrane-
70 associated NEU activation in murine or human macrophages and dendritic cells¹⁴. Upon

71 LPS binding to TLR4, NEU activity was shown to regulate NF- κ B induction in
72 macrophages, suggesting a role for this enzyme during cellular activation¹⁴.
73 Furthermore, in experimental Gram-negative sepsis or endotoxemia, NEU activity
74 mediated leukocyte dysfunction, associated with exacerbated inflammatory response
75 and high mortality rates^{15,16}. As previous studies have demonstrated that pathogen-
76 derived NEU stimulate neutrophils^{7,11,17}, we investigated whether endogenous host
77 NEUs can be targeted to regulate neutrophil dysfunction observed in severe infections.
78
79 Here, we have identified host NEU activation as a positive regulator of microbial-
80 induced human neutrophil overactivation. Additionally, we have employed the antiviral
81 NEU inhibitors Oseltamivir and Zanamivir to explore this pathway and found that these
82 drugs fine-tune the neutrophil dysfunction observed in sepsis and COVID-19. Together,
83 our results show that NEU is a potential target for the control of neutrophil dysfunction
84 and presenting Oseltamivir or Zanamivir as adjunctive therapy for severe infections.

85 **Results**

86

87 **LPS-induced surface Sia shedding in human neutrophils is mediated by NEU**
88 **activity**

89

90 As activated NEUs hydrolyze Sia residues linked to underlying galactose

91 glycoconjugates⁸, we employed a flow cytometry-based lectin binding assay to measure

92 Sia levels on neutrophils after their activation. Alpha2-3-Sia is a major functional Sia

93 linkage of surface glycans present on human neutrophils¹⁸. Therefore, we used the

94 lectin MAL-II that binds selectively to α 2-3- over α 2-6-linked Sia¹⁹. LPS treatment of

95 whole blood from healthy donors significantly reduces the binding of MAL-II on

96 neutrophils (CD66b⁺) when compared to untreated cells (**Supplementary Fig. 2A**).

97 Next, cells were stained with Fc-chimera of Siglec-9, a sialic acid-binding protein that

98 recognize Sia in α 2-3 and α 2-6 linkages²⁰. Similarly, we observed that binding of Siglec-

99 9-Fc (**Supplementary Fig. 2B**) is decreased on neutrophils treated with LPS,

100 confirming a reduction of neutrophil Sia residues likely due to LPS-induced NEU activity

101 in these cells. To test this hypothesis, we measured NEU activity in human leukocytes

102 using the NEU substrate 4-MU-NANA¹⁴ and validated the assay using NEU purified

103 from *C. perfringens* (CpNEU) (**Fig. 1A-B**). Both clinically available NEU inhibitors

104 Oseltamivir and Zanamivir reduce CpNEU activity (**Fig. 1A-B**). Using total leukocytes

105 from healthy donors, we observed that LPS-induced NEU activity was significantly

106 inhibited by Oseltamivir or Zanamivir (**Fig. 1C-D**). Moreover, these NEU inhibitors

107 prevent LPS- or CpNEU-mediated reduction of MAL-II binding on neutrophils surface

108 **(Fig. 1E-H)**. Together, these results show that LPS-induced host NEU activity
109 decreases Sia content on neutrophils, which can be inhibited by Oseltamivir and
110 Zanamivir.

111

112 **LPS-induced phagocytosis and killing of *E. coli* is modulated by NEU activity**

113

114 Bacteria uptake and killing are important functions of neutrophils⁴. We next investigated
115 whether host NEU regulates phagocytosis and killing of *E. coli*. Whole blood or total
116 leukocytes from healthy donors were preincubated with LPS or CpNEU, respectively,
117 and *E. coli* BioParticles® added to cells for 60 min. Ingested pHrodo *E. coli* by
118 neutrophils were analyzed by flow cytometry. As expected, we observed a significant
119 increase in MFI of pHrodo *E. coli* of unstimulated cells at 37 °C when compared to cells
120 at 4 °C (**Supplementary Fig. 3**). LPS (**Fig. 2A-C**) or CpNEU, used as a positive control
121 (**Fig. 2D-F**), but not heat-inactivated CpNEU, significantly enhances phagocytosis of *E.*
122 *coli*. Remarkably, these effects are inhibited by Zanamivir or Oseltamivir (**Fig. 2A-F**),
123 suggesting that LPS-enhanced phagocytosis involves a host NEU-dependent pathway.
124 Similarly, pretreatment of cells with LPS or CpNEU increases both the number of cells
125 with bacteria as well as the number of bacteria per cell (**Fig. 2G-J**). These effects were
126 also abolished when NEU inhibitors Oseltamivir and Zanamivir were added in the cell
127 cultures (**Fig. 2G-J**). Furthermore, LPS or CpNEU treatment enhances intracellular and
128 extracellular killing of *E. coli*, which are also inhibited by Oseltamivir or Zanamivir (**Fig.**
129 **2K-L**). These results suggest that NEU plays a critical role in LPS-stimulated
130 phagocytosis and killing responses of neutrophils.

131

132 **NEU blockade prevents neutrophil activation**

133 Shedding of cell surface Sia by mobilization of granule-associated NEU to the cell
134 surface has been associated with neutrophil activation²¹. Therefore, we analyzed
135 surface expression of CD66b and CD62L, two markers of human neutrophil activation²²⁻
136 ²⁴, and α 2-3-Sia levels in LPS-exposed whole blood cultures. Both Oseltamivir and
137 Zanamivir inhibit LPS-induced shedding of α 2-3-Sia (**Fig. 3A,B**) and CD62L (**Fig. 3D,E**)
138 or upregulation of CD66b (**Fig. 3G,H**) on neutrophils. Similarly, MAL-II preincubation,
139 which prevents hydrolysis of α 2-3-Sia by NEU²⁵ by steric hindrance at the NEU
140 cleavage site, blocks LPS-induced neutrophil activation (**Fig. 3C,F,I**). These data show
141 that dampening NEU activity or blocking the hydrolysis of α 2-3-Sia is sufficient to inhibit
142 human neutrophil activation by LPS. Similar results were observed in soluble CpNEU-
143 treated leukocytes (**Supplementary Fig. 4**). Next, we assessed whether NEU inhibitors
144 influenced LPS-stimulated ROS production and NETs release, key mediators of
145 bacterial killing and tissue injury²⁶. We observed that neutrophils primed with LPS and
146 stimulated with PMA produce higher amounts of ROS when compared to unprimed cells
147 (**Fig. 3J-L**). Both Oseltamivir and Zanamivir inhibit ROS release to levels similar to
148 unprimed cells. These results were also reproduced by the treatment of cells with
149 CpNEU (**Supplementary Fig. 5E-G**). Furthermore, Oseltamivir or Zanamivir
150 significantly inhibit LPS-induced NETs released by isolated neutrophils (**Fig. 3M**).
151 Together, these data indicate that microbial-induced host NEU activity regulates
152 important neutrophil functions *in vitro*.

153

154 **Oseltamivir enhances survival rate of mice in clinically relevant models of sepsis**

155 Exacerbated neutrophil responses such as increased ROS production, NETs release,
156 and degranulation are associated with tissue injury and organ dysfunction²⁷. By using
157 Oseltamivir as a therapeutic tool, we next explored the involvement of NEU activity *in*
158 *vivo* during experimental sepsis, a model of neutrophil dysfunction^{3,28,29}. We first
159 induced sepsis by intraperitoneal administration of 1×10^7 CFU/mice of the Gram-
160 negative *E. coli* (ATCC 25922), which lacks NEU in its genome³⁰. We used the dose of
161 10 mg/Kg of Oseltamivir by oral gavage (PO), which is the equivalent dose used in
162 humans (~ 7.5 mg/Kg)³¹. Oseltamivir pretreatment (2 hr before infection) plus post-
163 treatment (6 hr after infection, 12/12 h, PO, for 4 days) markedly boost host survival
164 **(Supplementary Fig. 6A)**. Only a single dose of Oseltamivir before (2 hr) bacterial
165 administration was sufficient to reduce disease pathology. Oseltamivir significantly
166 decreases the number of neutrophils in the BAL and lung tissue 4 or 6 hr after infection
167 **(Supplementary Fig. 6B-C)**. This pretreatment also augments the neutrophil migration
168 to the focus of infection, which is associated with an efficient control of infection
169 **(Supplementary Fig. 6D-F)**. Furthermore, pretreatment with Oseltamivir decreases
170 BAL and plasma TNF and IL-17 levels **(Supplementary Fig. 6G-J)** and tissue injury
171 markers (AST, ALT, ALP and total bilirubin) **(Supplementary Fig. 6K-N)**, as well as
172 prevents reduction of $\alpha 2$ -3-Sia on peritoneal lavage SSC^{high}/GR-1^{high} cells
173 **(Supplementary Fig. 6O-P)**. More importantly, the post-treatment efficacy of
174 Oseltamivir was also evaluated in survival of septic mice. Mice were IP challenged
175 with *E. coli* (1×10^7 CFU/mice) and treated 6 hr after infection with Oseltamivir for 4
176 days (10 mg/Kg, PO, 12/12h). Strikingly, in the post-treatment protocol, Oseltamivir

177 provides a significant improvement in the survival rate of septic mice (**Supplementary**
178 **Fig. 6Q**).

179

180 Next, we employed the CLP model to evaluate the effect of Oseltamivir in septic mice,
181 as it is considered the gold standard in preclinical sepsis³². Six hours after CLP, mice
182 were treated with Oseltamivir for 4 days (10 mg/Kg, PO, 12/12h). This treatment leads
183 to a small delay in the mortality rate of severe septic mice (**Fig. 4A**). Next, CLP septic
184 mice were treated with antibiotics because it is one of the standard interventions used in
185 clinical settings of sepsis³³. Importantly, compared to the control animals, therapeutic
186 use of Oseltamivir plus antibiotics drastically improved survival rates of CLP mice
187 (87.5% experimental group vs 25% control group) (**Fig. 4B**). Forty-eight hr after surgery,
188 post-treated septic mice have a significant reduction of neutrophils in BAL and lungs,
189 improvement of neutrophil migration at the focus of infection, and reduced bacterial load
190 in PL and blood (**Fig. 4C-G**). Levels of TNF and IL-17 in PL and plasma and tissue
191 injury markers were also reduced in Oseltamivir treated mice (**Fig. 4H-O**). Additionally,
192 Oseltamivir also leads to a higher expression of $\alpha 2$ -3-Sia on SSC^{high}/GR-1^{high} cells in PL
193 (**Fig. 4P-Q**) confirming blockade of NEU activity *in vivo*.

194

195 As respiratory tract infections, particularly pneumonia, are among the most common
196 sites of infection in sepsis³⁴, we intratracheally administered *K. pneumoniae* (ATCC
197 700603) into mice to address the effect of Oseltamivir. Post-treatment of mice with
198 Oseltamivir significantly improves survival of septic mice challenged with *K.*
199 *pneumoniae* (**Fig. 5A**). The increased host survival was accompanied by a decrease of

200 neutrophil migration in BAL, reduced levels of TNF and IL-17 and reduced levels of
201 tissue injury markers (**Fig. 5B-K**). Oseltamivir also prevents reduction of $\alpha 2$ -3-Sia on
202 BAL SSC^{high}/GR-1^{high} cells (**Fig. 5L-M**). Together, these results show that host NEU
203 activation exacerbates inflammatory responses during sepsis and the use of Oseltamivir
204 improves disease outcome.

205

206 **Oseltamivir and Zanamivir rescue overactivated neutrophils from COVID-19** 207 **patients**

208

209 Similar to bacterial sepsis, recent evidence suggests that neutrophils fuel hyper-
210 inflammatory response during severe SARS-CoV-2 infection. Larger numbers of
211 circulating neutrophils have been associated with poor prognosis of COVID-19 patients
212 and analysis of lung biopsies and autopsy specimens showed extensive neutrophil
213 infiltration^{2,35-41}. For instance, using single-cell analysis of whole blood from mild and
214 severe COVID-19 patients, Schulte-Schrepping *et al.* (2020) showed that neutrophils in
215 severe patients are highly activated, mainly characterized by the shedding of CD62L⁴².
216 Confirming previous findings, we observed that neutrophils from active COVID-19
217 patients, but not from convalescent patients, displayed shedding of CD62L (**Fig. 6A**)
218 and upregulation of CD66b (**Fig. 6B**), indicating a high activation state of these cells.
219 Moreover, neutrophils from severe COVID-19 patients were found to present a
220 significant reduction of surface $\alpha 2$ -3-Sia (**Fig. 6C**), suggesting that NEU activity is
221 increased during severe COVID-19. Therefore, we ask whether neuraminidase
222 inhibitors can rescue neutrophil activation from COVID-19 patients. *Ex vivo* treatment of

223 whole blood with Oseltamivir or Zanamivir decreased neutrophil activation and restored
224 the levels of cell surface $\alpha 2$ -3-Sia (**Fig. 6D-F**). **Fig. 6G** summarizes the effects of
225 Oseltamivir and Zanamivir on the surface levels of CD62L and $\alpha 2$ -3-Sia by neutrophils,
226 where these treatments lead to a formation of two different clusters in cells from severe
227 COVID-19 patients. As soluble NEU enzymes are also present in plasma¹⁵, we next
228 asked if plasma from COVID-19 patients can induce neutrophil response from healthy
229 donors. Indeed, stimulation of whole blood from healthy donors with fresh plasma from
230 severe, but not convalescent, COVID-19 patients leads to neutrophil activation (**Fig.**
231 **6H**), reduction of $\alpha 2$ -3-Sia (**Fig. 6I**) as well as ROS production (**Fig. 6J,K**), which were
232 significantly reduced by Oseltamivir or Zanamivir (**Fig. 6H-J**). Additionally, we observed
233 that activity of NEU is increased in plasma from severe COVID-19 patients
234 (**Supplementary Fig. 7A**). Serum glycoproteins from severe COVID-19 patients also
235 presented reduced levels of $\alpha 2$ -3-Sia (**Supplementary Fig. 7B-E**) suggesting NEU
236 activation *in vivo*. Moreover, plasma samples from severe COVID-19 patients that were
237 heat-inactivated to inhibit soluble NEU activity (**Supplementary Fig. 7F**) still induces
238 neutrophil activation, suggesting that cellular NEU in conjunction with circulating factors
239 mediate NEU-dependent neutrophil activation in severe COVID-19. These results
240 highlight host NEU as a regulator of neutrophil activation in severe COVID-19 and
241 suggest this pathway as a potential host-directed intervention target to rewire neutrophil
242 responses during severe disease.

243 **DISCUSSION**

244

245 Systemic inflammatory response may lead to unsuitable neutrophil stimulation, which is
246 associated with higher mortality rates in sepsis and sepsis-like diseases⁴³. Therefore,
247 finding new therapeutic options to prevent neutrophil overstimulation while maintaining
248 their microbicidal abilities is hugely desired. Neuraminidase inhibitors are promising
249 drugs to fill this gap. Here we demonstrated that endogenous host NEUs mediate
250 exacerbated inflammatory responses by primary neutrophils. Clinically used viral NEU
251 inhibitors, Oseltamivir and Zanamivir, decrease human NEU activity and are effective in
252 prevent LPS-induced neutrophil responses or to rescue overactivation of neutrophils
253 from COVID-19 patients. In severe murine sepsis, therapeutic use of Oseltamivir fine-
254 tunes neutrophil migration results in bacterial clearance and high survival rates.

255

256 All of the four different isotypes of NEU described in mammals (NEU1, NEU2, NEU3
257 and NEU4) remove Sia from glycoproteins and glycolipids with specific substrate
258 preferences⁴⁴. NEU1 cleaves preferentially α 2-3-Sia and seems to be the most
259 important isoenzyme in immune cells. NEU1 is a lysosomal enzyme but it is also
260 present at the cell surface where it can regulate multiple receptors such as Fc gamma
261 receptor (Fc γ R), insulin receptor, integrin β -4, and TLRs⁴⁵. While several stimuli were
262 described to induce NEU activity including LPS¹⁴, PMA, calcium ionophore A23187,
263 fMLP²¹, and IL-8⁴⁶, how NEUs are activated is poorly understood. However, NEU1
264 activation involves formation of a multicomplex of enzymes that stabilizes NEU1 in its
265 conformational active state⁴⁷. Interestingly, NEU1 was found to be associated with

266 matrix metalloproteinase-9 (MMP9) at the surface of naive macrophages⁴⁸. LPS binding
267 to TLR4 leads to activation of a G protein-coupled receptor (GPCR) via Gai subunit and
268 MMP9 to induce NEU1 activity, which in turn removes α 2-3-Sia from TLR4, allowing its
269 dimerization and intracellular signaling^{25,48,49}. Although we have not formally addressed
270 whether the LPS-TLR4 pathway directly activates NEU function in human neutrophils,
271 our results employing MAL-II preincubation suggest desialylation is required for LPS-
272 mediated neutrophil responses. Thus, it is possible that NEU controls Sia levels in TLR4
273 molecules in human neutrophils as observed in macrophages and dendritic cells^{25,49}.
274 The effects of LPS on neutrophil responses observed here are in accordance with the
275 well-documented induction of ROS and NETs as well as in phagocytosis and bacterial
276 killing by these phagocytes⁵⁰⁻⁵⁴. Importantly, the upstream involvement of NEU
277 regulating LPS responses by neutrophils is in agreement with the previous
278 demonstration that TLRs stimulate these cells independent of gene transcription⁵⁰.
279 Together, our data suggests that NEU activation provides a fast response to enhance
280 microbial-induced neutrophil functions. Thus, we speculate that this could be an
281 evolutionary mechanism by which neutrophils quickly mobilize their microbicidal
282 mediators against pathogens.

283

284 Sialic acid removal from neutrophils surface markedly changes their adhesiveness,
285 chemotaxis, and migration^{21,55-58}. In peritonitis- or pneumonia-induced sepsis in mice,
286 we observed that Oseltamivir prevented the massive neutrophil infiltration into
287 bronchoalveolar spaces or lung tissues, suggesting that regulation of neutrophil
288 migration by dampening NEU activity contributes to survival of septic mice. Interestingly,

289 we observed a divergent effect of Oseltamivir on neutrophil migration to the focus of
290 infection between peritonitis- and pneumonia-induced sepsis. This could be explained
291 by the different mechanisms involved in neutrophil migration to the peritoneal cavity and
292 lungs. While expression of CD62L and rolling of neutrophils to endothelium is necessary
293 for its migration to the peritoneal cavity, it seems to be not required for migration into the
294 lungs^{3,59}. Moreover, systemic neutrophil activation leads to cell stiffening, resulting in
295 retention of neutrophils in the small capillaries of the lungs⁶⁰, which is frequently the first
296 organ impaired in non-pneumonia- and pneumonia-induced sepsis⁶¹. The role of NEU-
297 induced neutrophil activation suggested here is in agreement with previous
298 demonstration that NEU1 deletion in hematopoietic cells confers resistance to
299 endotoxemia¹⁶. Also, the sialidase inhibitor Neu5Gc2en protects endotoxemic irradiated
300 wild-type (WT) mice reconstituted with WT bone marrow but not WT mice reconstituted
301 with NEU1^{-/-} bone marrow cells¹⁶. Similar to our finds, the treatment of mice with NEU
302 inhibitors increases host survival in *E. coli*-induced sepsis¹⁵. This outcome was
303 correlated with significant inhibition of blood NEU activity. Enhancement of soluble NEU
304 activity in serum decreases the Sia residues from alkaline phosphatase (APL) enzymes,
305 which are involved in the clearance of circulating LPS-phosphate during sepsis¹⁵.
306
307 SARS-CoV-2 infection leads to mild illness in most of the patients, but ~20% of them
308 progress to severe disease with many characteristics resembling sepsis, including acute
309 respiratory distress syndrome (ARDS), cytokine storm, and neutrophil dysregulation^{38,62–}
310 ⁶⁴. The transcriptional programs found in neutrophil subsets from blood and lungs of
311 severe, but not mild, COVID-19 patients are related to cell dysfunction, coagulation, and

312 NETs formation^{39,42}. We observed that blood neutrophils from severe COVID-19 are
313 highly activated as demonstrated by reduced CD62L expression and increase of CD66b
314 expression, as previously reported⁴². We now add new information by showing that
315 neutrophils from severe, but not convalescent, COVID-19 patients have reduced
316 surface levels of α 2-3-Sia, suggesting a relevant role of NEU for neutrophil activation
317 during COVID-19. More importantly, both the NEU inhibitors Oseltamivir and Zanamivir,
318 increased the α 2-3-Sia content and rewired the overactivation of neutrophils from
319 severe COVID-19 patients. We speculate that the addition of NEUs competitive
320 inhibitors allowed the endogenous sialyltransferases to restore sialyl residues on
321 surface glycoconjugates. Fast changes of surface sialic acid levels by sialidases and
322 sialyltransferases seems to be an important mechanism to control neutrophil
323 response⁵⁵. In neutrophils from healthy donors or COVID-19 convalescent patients,
324 Oseltamivir and Zanamivir did not interfere in resting state and had no effect on α 2-3-
325 Sia content, suggesting that NEU has a low effect on surface Sia turnover on non-
326 activated neutrophils. How neutrophils are activated and the role of NEU in this process
327 remains to be defined in COVID-19, nevertheless, recent evidence showed that
328 neutrophils could be directly activated by SARS-CoV-2², cytokines⁶⁵, and alarmins^{39,42}
329 such as calprotectin³⁹, a TLR4 ligand⁶⁶. In addition, we now add new evidence by
330 showing that soluble NEU together with other circulating factors present in plasma from
331 severe COVID-19 patients also accounts for neutrophil activation.

332

333 Collectively, this work suggests that host NEU activation leads to shedding of surface
334 sialic acid with consequent neutrophil overstimulation, tissue damage, and high

335 mortality rates. On the other hand, NEU inhibitors-prevented shedding of sialic acid and
336 regulates neutrophil response, resulting in infection control and high survival rates
337 (working model in **Supplementary Fig. 8**). Taking into account that both drugs are
338 broadly used in humans with well-known toxic and adverse effects, our data suggest
339 Oseltamivir and Zanamivir could be repurposed for the treatment of sepsis or severe
340 infections such as COVID-19. Interestingly, a retrospective single-center cohort study
341 including 1190 patients with COVID-19 in Wuhan, China, showed that administration of
342 Oseltamivir was associated with a decreased risk of death in severe patients⁶⁷. Our data
343 suggest that such encouraging results may be explained by the inhibition of NEU-
344 mediated neutrophil dysfunction *in vivo*. Nevertheless, randomized clinical trials with
345 clinically used NEU inhibitors in sepsis and COVID-19 are required to directly explore
346 this hypothesis.

347 **MATERIALS AND METHODS**

348

349 **Human blood samples**

350

351 Blood was collected from healthy donors (25 - 45 yr old, n=3-12) in endotoxin-free tubes
352 with K₃EDTA (Labor Import, Brasil). All participants gave their written informed consent
353 for blood collection after been informed on procedures. The research protocol followed
354 the World Medical Association Declaration of Helsinki and was approved by the
355 Institutional Review Board of the Federal University of Santa Catarina (CAAE
356 #82815718.2.0000.0121). Blood samples were also collected from severe COVID-19
357 (n=6) or convalescent COVID-19 (n=8) patients (25 to 89 yr old) admitted in the
358 Intensive Care Unit (ICU) or NUPAIVA (Research Center on Asthma and Airway
359 Inflammation) at the UFSC University Hospital from August to October 2020. Blood
360 samples from sex-matched healthy donors were used as controls. All patients or a close
361 family member gave consent for participation in the study, which was approved by the
362 UFSC IRB (CAAE #36944620.5.1001.0121). Supplementary Table 1 summarizes
363 patients clinical and laboratory records. These samples were used to analyze neutrophil
364 activation, surface α 2-3-Sia as well as the effect of plasma under these parameters and
365 ROS production. Blood samples were also collected from severe COVID-19 (n=5)
366 patients (55 to 73 yr old) admitted at the Hospital Naval Marcílio Dias (HNMD). The
367 research was approved by the Research Ethics Committee (CEP) from Brazilian
368 National Health Council. All patients signed a free and informed consent form following
369 current legislation and the relevant ethical regulations approved by the Hospital Naval

370 Marcílio Dias (CAAE #31642720.5.0000.5256). These samples were used to analyze
371 the sialylation of plasma proteins. Supplementary Table 2 summarizes the clinical and
372 laboratory information of patients from this cohort.

373

374 **Evaluation of neutrophil activation, phagocytosis, killing, ROS, and NETs release**

375

376 Whole blood containing 1×10^6 leukocytes were incubated (37°C , 5% CO_2) in the
377 presence or absence of Oseltamivir (100 μM , Sigma-Aldrich, San Luis, MO, USA),
378 Zanamivir (30 μM , Sigma-Aldrich), LPS (1 $\mu\text{g}/\text{mL}$, *E. coli* 0127:b8, Sigma-Aldrich), LPS
379 plus Oseltamivir or LPS plus Zanamivir for 90 min. Concentrations of Oseltamivir and
380 Zanamivir used here were chosen by concentration-effect experiments (10-100 μM
381 Oseltamivir and 1-30 μM Zanamivir) (data not shown). Since plasma is a rich source of
382 glycoconjugates, total leukocytes were used instead of whole blood to evaluate the
383 effect of isolated neuraminidase from *Clostridium perfringens* (CpNEU) on neutrophils.
384 Red blood cells (RBCs) were lysed by lysis buffer (0.15 M NH_4Cl ; 0.1 mM EDTA; 12 mM
385 Na_2HCO_3) for 7 min, RT, followed by centrifugation (270 x g; 22°C ; 7 min). Total
386 leukocytes (1×10^6 cells) were incubated (37°C , 5% CO_2) in the presence or absence
387 of CpNEU (10 mU, Sigma-Aldrich), CpNEU plus Oseltamivir (100 μM) or CpNEU plus
388 Zanamivir (30 μM) for 60 min. Next, the following assays were performed. Analysis of
389 neutrophil activation. Leukocytes were then washed and resuspended in FACS buffer (2
390 mM EDTA/PBS). The mix of antibodies against CD66b (G10F5; BioLegend, San Diego,
391 CA, USA), CD62L (DREG-56; BioLegend), CD16 (3G8; BioLegend), isotypes or
392 *Maackia amurensis* Lectin II biotinylated (MAL-II, Vector Labs, San Diego, CA, USA)

393 coupled to Streptavidin (Biolegend), plus human BD Fc Block™ (BD Pharmingen™) and
394 Fixable Viability Stain (FVS, BD Horizon™, San Jose, CA, USA) were added to
395 leukocytes for 30 min at 4 °C. Cells were washed, resuspended in FACS buffer,
396 acquired in a FACSVerse cytometer and analyzed using FlowJo software (FlowJo LLC).
397 Approximately 100.000 gated events were acquired in each analysis. Phagocytosis
398 assays. After RBCs lysis, 1×10^6 leukocytes were incubated at 37 °C (5% CO₂) or at 4
399 °C (control) with 100 µg/mL pHrodo™ Red *E. coli* BioParticles® (Thermo Fisher,
400 Waltham, MA, USA) for 60 min and the MFI of neutrophils (FVS⁻/CD66b⁺ cells) with
401 ingested bioparticle was analyzed by FACS. Total leukocytes were also incubated with
402 1×10^6 CFU of live *E. coli* (ATCC 25922) for 90 min (37 °C, 5% CO₂). Next, the cells
403 were washed twice (2 mM EDTA/PBS), fixed (FACS buffer/PFA 2%) and the
404 percentage of neutrophils with bacteria or the percentage of neutrophils with ≥ 3 bacteria
405 was analyzed by light microscopy using Differential Quick Stain Kit (Laborclin, Brazil).
406 Bacterial killing. Total leukocytes (1×10^6) were incubated (37 °C, 5% CO₂) with 1×10^6
407 CFU of live *E. coli* for 180 min. The samples were centrifuged (270 g, 7 min, 4 °C) and
408 10 µL of supernatant were diluted until 10^6 and spread onto agar brain-heart infusion
409 (BHI, Kasvi, Brazil) to quantify the viable extracellular bacteria. The pellets were washed
410 twice with PBS/2 mM EDTA (270 g, 7 min, 4 °C), the leukocytes were lysed with 2%
411 Triton-X, washed (PBS, 2000 g, 15 min, 4 °C), resuspended in PBS and 10 µL of
412 samples were diluted until 10^6 and spread onto agar BHI. Plates were incubated
413 overnight at 37 °C and viable bacteria were expressed as mean \pm SEM of CFU/mL.
414 ROS assay. After RBCs lysis, 1×10^6 leukocytes were incubated at 37 °C (5% CO₂) with
415 10 µM of cell-permeant 2',7'-dichlorodihydrofluorescein diacetate (CM-H2DCFDA,

416 ThermoFisher) for 5 min. Next, cells were stimulated or not with phorbol 12-myristate
417 13-acetate (PMA) for 10 min, fixed, washed twice with PBS/2 mM EDTA (270 g, 7 min,
418 4 °C) and analyzed by FACS. *NETs assay*. NETs quantification was performed as
419 previous described⁶⁸ on the supernatant of isolated neutrophils. Briefly, an anti-MPO
420 antibody bound to a 96-well flat-bottom plate captured the enzyme MPO (5 µg/ml;
421 Abcam), and the amount of DNA bound to the enzyme was quantified using the Quant-
422 iT™ PicoGreen® kit (Invitrogen, Carlsbad, CA, USA) according to the manufacturer's
423 instructions. Fluorescence intensity (Ex 488 nm/Em 525 nm) was quantified in a
424 FlexStation 3 Microplate Reader (Molecular Devices, San Jose, CA, USA). *Neutrophil*
425 *isolation*. Human circulating neutrophils were isolated by Percoll density gradients⁶⁹.
426 Briefly, four different gradients, 72%, 65%, 54%, and 45%, were used to isolate human
427 circulating neutrophils. After centrifugation at 600 g for 30 min at 4 °C, the cell layer at
428 the 72% gradient interface was collected as the neutrophil fraction. The erythrocytes
429 were removed by lysis, and cell pellets were resuspended in RPMI 1640. Isolated
430 neutrophils (1 x 10⁶/well) were treated with Oseltamivir, Zanamivir or medium 1 h before
431 the stimulus with PMA (50 nM) or LPS (10 µg/mL). After 4 hr of stimuli (37 °C, 5% CO₂),
432 the supernatant was collected to measure the levels of NETs.

433

434 **Neutrophil responses with plasma from COVID-19 patients**

435

436 Whole blood samples from sex-matched healthy donors (n = 7) were incubated for 2 h
437 (37 °C, 5% CO₂) with 7% of fresh plasma from healthy donors, severe or convalescent
438 COVID-19 patients or heat-inactivated plasma (56 °C, 30 min) from severe COVID-19

439 patients in the presence or absence of Oseltamivir (100 μ M) or Zanamivir (30 μ M).

440 Surface levels of α 2-3-Sia and CD66b and ROS production were assessed on

441 neutrophils by FACS.

442

443 **Neuraminidase kinetics assay**

444

445 After RBCs lysis, 0.5×10^6 leukocytes were resuspended in HBSS and added to 96-well

446 flat-bottom dark plate (SPL Life Sciences, South Korea) on ice. Then, 4-

447 Methylumbelliferyl-N-acetyl- α -D-Neuramic Acid (4-MU-NANA, Sigma-Aldrich) substrate

448 (0.025 mM) was added followed by medium, or LPS (1 μ g/mL), LPS plus Oseltamivir

449 (100 μ M), LPS plus Zanamivir (30 μ M). CpNEU (10 mU), CpNEU plus Oseltamivir or

450 CpNEU plus Zanamivir were used as positive controls of the assay. The volume was

451 completed to 200 μ L with HBSS, followed by reading on the Spectramax® Paradigm®

452 instrument starting 3 min after and every 5 min for 55 min at 37 °C. Sialidase activity

453 was also assessed in heat-inactivated or fresh plasma from severe COVID-19 patients

454 in the presence or absence of Oseltamivir (100 μ M) or Zanamivir (30 μ M) using Tecan

455 Infinite 200 multi-reader. The fluorescent substrate 4-MU-NANA formation was detected

456 at ex 350 nm/em 450 nm.

457

458 **Mice**

459

460 The care and treatment of the animals were based on the Guide for the Care and Use

461 of Laboratory Animals⁷⁰ and all procedures followed the ARRIVE guidelines and the

462 international principles for laboratory animal studies⁷¹. C57BL/6 (Jackson Laboratory,
463 Bar Harbor, ME, USA) mice (8–10 weeks old) and Swiss mice (10–12 weeks old) were
464 housed in cages at $21 \pm 2^\circ\text{C}$ with free access to water and food at the Animal Facility of
465 the Department of Microbiology, Immunology, and Parasitology and Department of
466 Pharmacology from UFSC, respectively. A total of 228 mice were used in this study.
467 Protocols were approved by the Animal Use Ethics Committee of UFSC (CEUA
468 #8278290818).

469

470 ***E. coli*-, *Klebsiella pneumoniae*- and CLP-induced sepsis**

471

472 *E. coli* (ATCC 25922, Manassas, VA, USA) or *K. pneumoniae* (ATCC 700603) were
473 used to induce severe sepsis in mice. Naive mice were intraperitoneal (IP) challenged
474 with 100 μL of 1×10^7 CFU of the *E. coli* suspension. A group of *E. coli*-septic mice was
475 randomly pretreated (2 hr before infection) and post treated by *per oral* (PO, 12/12 hr)
476 via with saline or Oseltamivir phosphate (10 mg/kg, Eurofarma, Brazil) for 4 days to
477 survival analysis. Another group was pretreated 2 hr before infection with a single dose
478 of Oseltamivir phosphate (10 mg/kg, PO) and the pathophysiological response was
479 analyzed at 4 and 6 hr after infection. *E. coli*-septic mice were also randomly
480 posttreated (6 hr after infection, 12/12 hr) with saline or Oseltamivir phosphate (PO, 10
481 mg/kg) for 4 days to survival analysis. For pneumonia-induced sepsis, mice were
482 anesthetized with isoflurane (3–5 vol%) and placed in supine position. A small incision
483 was made in the neck where the trachea could be localized and a *K. pneumoniae*
484 suspension (4×10^8 CFU/50 μL of PBS) was injected into the trachea with a sterile 30-

485 gauge needle. Skin was sutured and animals were left for recovery in a warm cage.
486 After 6 hr of infection and then 12/12 hr mice were treated with Oseltamivir phosphate
487 (PO, 10 mg/kg) for survival analysis. In another set of experiments, pneumonia was
488 induced and mice were treated 6 hr after infection with a single dose of Oseltamivir
489 phosphate (10 mg/kg, PO) for material collection and analysis of pathophysiological
490 response 24 hr after infection.

491 Cecal ligation and puncture (CLP)-induced sepsis were performed as previously
492 described²⁸. Mice were anesthetized with xylazine (2 mg/kg, IP, Syntec, Brazil) followed
493 by isoflurane (3–5 vol%, BioChimico, Brazil), a 1 cm midline incision was made in the
494 anterior abdomen, and the cecum was exposed and ligated below the ileocecal junction.
495 The cecum was punctured twice with an 18-gauge needle and gently squeezed to allow
496 its contents to be released through the punctures. Sham-operated (Sham) animals
497 underwent identical laparotomy but without cecal ligation and puncture. The cecum was
498 repositioned in the abdomen, and the peritoneal wall was closed. All animals received 1
499 mL of 0.9% saline subcutaneous (SC) and 100 µL of tramadol (5 mg/kg, SC, Vitalis,
500 Brazil) immediately after CLP. CLP-septic mice were randomly treated (starting 6 h after
501 infection, PO) with 100 µL of saline or Oseltamivir phosphate (10 mg/kg, 12/12 hr) for 4
502 days. In another set of experiments, CLP mice were randomly IP treated (6 hr after
503 infection, 12/12 hr) during 4 days with 100 µL metronidazole (15 mg/kg, Isofarma,
504 Brazil) plus ceftriaxone (40 mg/kg, Eurofarma, Brazil) and Oseltamivir phosphate (10
505 mg/kg) or saline by PO to survival analysis or treated for 36 hr to analyze the
506 pathophysiological response at 48 hr after CLP.

507 **Neutrophil migration**

508 The animals were euthanized in a CO₂ chamber, the bronchoalveolar lavage (BAL) and
509 peritoneal lavage (PL) were performed and the number of neutrophils was determined
510 at 4 and 6 hr after *E. coli*, 24 hr after *K. pneumoniae* infection or 48 hr after CLP
511 surgery, as described²⁸. Next, mice were perfused with PBS/EDTA (1 mM) and the
512 lungs were harvested. Lungs were passed through 40- μ m nylon cell strainers and
513 single-cell suspensions were centrifuged in 35% Percoll® solution (315 mOsm/kg,
514 Sigma-Aldrich) for 15 min at 700 g to enrich leukocytes populations. Pelleted cells were
515 then collected, and erythrocytes were lysed. Single-cell suspensions from individual
516 mice were determined using a cell counter (Coulter ACT, Beckman Coulter, Brea, CA,
517 USA) or with a haemocytometer. Differential counts were also determined on Cytospin
518 smears stained using Differential Quick Stain Kit (Laborclin, Brazil). Blood samples were
519 collected by heart puncture and tubes containing heparin for further analysis.
520 Neutrophils from LP or BAL were also stained with anti-Ly-6G/Ly-6C (GR-1, RB6-8C5;
521 BioLegend) and MAL-II to be further analyzed by FACS, as previously described.
522 Analysis was carried out in SSC^{high}/GR-1^{high} cells.

523 **Bacterial counts**

524 The bacterial counts were determined as previously described²⁸. Briefly, the BAL, PL or
525 blood were harvested and 10 μ L of samples were plated on Muller-Hinton agar dishes
526 (Difco Laboratories, Waltham, MA, USA) and incubated for 24 hr at 37 °C. PL or BAL
527 samples were diluted until 10⁶.

528 **ELISA**

529 TNF (R&D Systems, Minneapolis, MN, USA) and IL-17 (XpressBio Life Sciences
530 Products, Frederick, MD, USA) levels in plasma, PL or BAL were determined by ELISA
531 kits according to the manufacturer's instructions.

532 **Tissue injury biochemical markers**

533 Aspartate aminotransferase (AST), alanine aminotransferase (ALT), alkaline
534 phosphatase (ALP) activities, and the levels of total bilirubin were determined in plasma
535 samples by commercial kits (Labtest Diagnóstica, Brazil). The procedures were carried
536 out according to the manufacturer's instructions.

537

538 **Lectin blotting of serum glycoproteins**

539 To evaluate if severe COVID-19 changes the α 2-3 sialylation of serum glycoproteins,
540 serum samples from four healthy donors and five severe COVID-19 patients were
541 blotted with MAL-II as previously described⁷². Samples were diluted in SDS-PAGE
542 sample buffer and heated at 100 °C for 5 min. Twelve μ g of total protein were resolved
543 in 10% SDS-PAGE and transferred onto nitrocellulose membranes (Millipore,
544 Burlington, MA, USA). Membranes were blocked (TBST + 5% BSA) overnight at 4 °C
545 and incubated for 2 hr with 1 μ g/mL of biotin-conjugated MAL-II, washed and incubated
546 for 40 min with alkaline-phosphatase (ALP)-conjugated streptavidin (Southern Biotec,
547 Birmingham, AL, USA) diluted 1:10.000. Both MAL-II and streptavidin-ALP were diluted
548 in TBST (5% BSA plus 150 mM of CaCl₂). Membranes were then revealed with

549 BCIP/NBT (5-bromo-4-chloro-3-indolyl-phosphate/nitro blue tetrazolium) color
550 development substrate (Promega, Brazil). The lane intensities were quantified using the
551 Image J software. In parallel, the resolved SDS-PAGE were stained with Coomassie
552 Brilliant blue R 250 (Merck KGaA, Germany) to compare the protein profile between the
553 different samples.

554

555 **Statistical analysis**

556 The data are reported as the mean or median \pm SEM of the values obtained from two to
557 seven independent experiments. Each experiment using human samples was
558 performed using three to five samples from healthy donors or one to three samples from
559 severe or convalescent COVID-19 patients. We used five mice per experimental group
560 except for survival analyses in which twelve to twenty mice were used. The mean or
561 median values for the different groups were compared by analysis of variance (ANOVA)
562 followed by Dunnett and/or Tukey post-tests. Bacterial counts were analyzed by the
563 Mann–Whitney *U*-test or unpaired *t*-test using a parametric test with Welch's correction.
564 Survival curves were plotted using the Kaplan–Meier method and then compared using
565 the log-rank method and Gehan-Wilcoxon test. Data was analyzed using GraphPad
566 Prism version 8.00 for Mac (GraphPad Software, USA). A $P < 0.05$ was considered
567 significant.

568 **Abbreviations**

- 569 4-MU-NANA 4-methylumbelliferyl-N-acetyl- α -D-Neuramic Acid
- 570 ALP alkaline phosphatase
- 571 ALT alanine aminotransferase
- 572 ARRIVE Animal Research: Reporting of In Vivo Experiments
- 573 AST aspartate aminotransferase
- 574 ATCC American Type Culture Collection
- 575 BAL bronchoalveolar lavage
- 576 BHI brain–heart infusion
- 577 CD cluster of differentiation
- 578 CFU colony forming units
- 579 CLP cecal ligation and puncture
- 580 CM-H2DCFDA cell-permeant 2',7'-dichlorodihydrofluorescein diacetate
- 581 CpNEU *Clostridium perfringens* neuraminidase
- 582 DANA 2,3-dehydro-2-deoxy-N-acetylneuraminic acid
- 583 EDTA ethylenediamine tetra-acetic acid
- 584 FACS fluorescence-activated cell sorting

- 585 FcγR Fc gamma receptor
- 586 fMLP N-formyl-Met-Leu-Phe
- 587 FVS fixable viability stain
- 588 HBSS Hanks' balanced salt solution
- 589 IgG immunoglobulin G
- 590 IP intraperitoneal pathway
- 591 LPS lipopolysaccharide
- 592 MAL-II *Maackia amurensis* lectin II
- 593 MFI median fluorescence intensity
- 594 NETs neutrophil extracellular traps
- 595 NEU neuraminidases
- 596 Neu5Ac2en 2-deoxy-2, 3-didehydro-D-N-acetylneuraminic acid
- 597 PBS phosphate buffered saline
- 598 PFA paraformaldehyde
- 599 PL peritoneal lavage
- 600 PMA 12-myristate 13-acetate
- 601 PMN polymorphonuclear

- 602 PO oral pathway
- 603 RBCs red blood cells
- 604 ROS reactive oxygen species
- 605 SARS-CoV-2 severe acute respiratory syndrome coronavirus 2
- 606 SC subcutaneous pathway
- 607 Sia sialic acids
- 608 Siglecs sialic acid-binding immunoglobulin-like lectins
- 609 TLR toll-like receptor
- 610 COVID-19 coronavirus disease 2019
- 611 WT wild-type

612 **Acknowledgments**

613 We thank UFSC microscopy (LCME) and biology (LAMEB) facilities for technical
614 support.

615

616 **Authors' contributions**

617 All named authors meet the criteria of Nature Medicine for authorship of this manuscript,
618 take responsibility for the work's integrity as a whole, and have given final approval for
619 publication.

620

621 ROF, FCA, DM, RS, DSM, AB, MSM and FS designed experiments and analyzed data;
622 ROF, FAC, CFS, DM, CWW, CLB, AAS, JA, LFF, CCN, NMP, PCS, FRF, FAS, LA, NH,
623 AB and FS performed experiments; SB, AM, MSM, FQC and RM contributed with
624 critical reagents/tools/clinical samples; ROF, FS, AB wrote the manuscript.

625

626 **Competing Interests statement**

627 The authors declare that no conflict of interest exists.

628

629 **Funding**

630 This work was funded by FAPESP-SCRIPPS (FS; 15/50387-4), Howard Hughes
631 Medical Institute – Early Career Scientist (AB; 55007412), National Institutes of Health
632 Global Research Initiative Program (AB; TW008276), CAPES Computational Biology
633 (DSM; 23038.010048/2013–27), CNPQ/COVID-19 (AB; 401209/2020-2), CNPQ/PQ
634 Scholars (AB and DSM), FAPESC Scholarship (DM).

635 References

- 636 1. Mócsai, A. Diverse novel functions of neutrophils in immunity, inflammation, and beyond. *J.*
637 *Exp. Med.* **210**, 1283–1299 (2013).
- 638 2. Veras, F. P. *et al.* SARS-CoV-2-triggered neutrophil extracellular traps mediate COVID-19
639 pathology. *J. Exp. Med.* **217**, (2020).
- 640 3. Alves-Filho, J. C., Spiller, F. & Cunha, F. Q. Neutrophil paralysis in sepsis. *Shock* **34 Suppl**
641 **1**, 15–21 (2010).
- 642 4. Segal, A. W. How neutrophils kill microbes. *Annu. Rev. Immunol.* **23**, 197–223 (2005).
- 643 5. Steevels, T. A. M. & Meyaard, L. Immune inhibitory receptors: essential regulators of
644 phagocyte function. *Eur. J. Immunol.* **41**, 575–587 (2011).
- 645 6. Macauley, M. S., Crocker, P. R. & Paulson, J. C. Siglec-mediated regulation of immune cell
646 function in disease. *Nat. Rev. Immunol.* **14**, 653–666 (2014).
- 647 7. Chang, Y.-C., Uchiyama, S., Varki, A. & Nizet, V. Leukocyte inflammatory responses
648 provoked by pneumococcal sialidase. *MBio* **3**, (2012).
- 649 8. Varki, A. Sialic acids in human health and disease. *Trends. Mol. Med.* **14**, 351–360 (2008).
- 650 9. Lipničánová, S., Chmelová, D., Ondrejovič, M., Frečer, V. & Miertuš, S. Diversity of
651 sialidases found in the human body - A review. *Int. J. Biol. Macromol.* **148**, 857–868 (2020).
- 652 10. Varki, A. & Gagneux, P. Multifarious roles of sialic acids in immunity. *Ann. N. Y. Acad. Sci.*
653 **1253**, 16–36 (2012).
- 654 11. Suzuki, H., Kurita, T. & Kakinuma, K. Effects of neuraminidase on O₂ consumption and
655 release of O₂ and H₂O₂ from phagocytosing human polymorphonuclear leukocytes. *Blood*
656 **60**, 446–453 (1982).
- 657 12. Arora, D. J. S. & Henrichon, M. Superoxide Anion Production in Influenza Protein-Activated
658 NADPH Oxidase of Human Polymorphonuclear Leukocytes. *J. Infect. Dis.* **169**, 1129–1133
659 (1994).

- 660 13. Henricks, P. A., van Erne-van der Tol, M. E. & Verhoef, J. Partial removal of sialic acid
661 enhances phagocytosis and the generation of superoxide and chemiluminescence by
662 polymorphonuclear leukocytes. *J. Immunol.* **129**, 745–750 (1982).
- 663 14. Amith, S. R. *et al.* Dependence of pathogen molecule-induced Toll-like receptor activation
664 and cell function on Neu1 sialidase. *Glycoconj. J.* **26**, 1197–1212 (2009).
- 665 15. Yang, W. H. *et al.* Accelerated Aging and Clearance of Host Anti-inflammatory Enzymes by
666 Discrete Pathogens Fuels Sepsis. *Cell. Host. Microbe.* **24**, 500–513.e5 (2018).
- 667 16. Chen, G.-Y. *et al.* Broad and direct interaction between TLR and Siglec families of pattern
668 recognition receptors and its regulation by Neu1. *Elife* **3**, e04066 (2014).
- 669 17. Mills, E. L., Debets-Ossenkopp, Y., Verbrugh, H. A. & Verhoef, J. Initiation of the respiratory
670 burst of human neutrophils by influenza virus. *Infect. Immun.* **32**, 1200–1205 (1981).
- 671 18. Mondal, N. *et al.* ST3Gal-4 is the primary sialyltransferase regulating the synthesis of E-, P-
672 , and L-selectin ligands on human myeloid leukocytes. *Blood* **125**, 687–696 (2015).
- 673 19. Knibbs, R. N., Goldstein, I. J., Ratcliffe, R. M. & Shibuya, N. Characterization of the
674 carbohydrate binding specificity of the leucoagglutinating lectin from *Maackia amurensis*.
675 Comparison with other sialic acid-specific lectins. *J. Biol. Chem.* **266**, 83–88 (1991).
- 676 20. Movsisyan, L. D. & Macauley, M. S. Structural advances of Siglecs: insight into synthetic
677 glycan ligands for immunomodulation. *Org. Biomol. Chem.* **18**, 5784–5797 (2020).
- 678 21. Cross, A. S. & Wright, D. G. Mobilization of sialidase from intracellular stores to the surface
679 of human neutrophils and its role in stimulated adhesion responses of these cells. *J. Clin.*
680 *Invest.* **88**, 2067–2076 (1991).
- 681 22. Schmidt, T. *et al.* CD66b overexpression and homotypic aggregation of human peripheral
682 blood neutrophils after activation by a gram-positive stimulus. *J. Leukoc. Biol.* **91**, 791–802
683 (2012).
- 684 23. Kishimoto, T. K., Jutila, M. A., Berg, E. L. & Butcher, E. C. Neutrophil Mac-1 and MEL-14
685 adhesion proteins inversely regulated by chemotactic factors. *Science* **245**, 1238–1241

- 686 (1989).
- 687 24. Jutila, M. A., Rott, L., Berg, E. L. & Butcher, E. C. Function and regulation of the neutrophil
688 MEL-14 antigen in vivo: comparison with LFA-1 and MAC-1. *J. Immunol.* **143**, 3318–3324
689 (1989).
- 690 25. Amith, S. R. *et al.* Neu1 desialylation of sialyl alpha-2,3-linked beta-galactosyl residues of
691 TOLL-like receptor 4 is essential for receptor activation and cellular signaling. *Cell. Signal.*
692 **22**, 314–324 (2010).
- 693 26. Mittal, M., Siddiqui, M. R., Tran, K., Reddy, S. P. & Malik, A. B. Reactive oxygen species in
694 inflammation and tissue injury. *Antioxid. Redox Signal.* **20**, 1126–1167 (2014).
- 695 27. Sônego, F. *et al.* Paradoxical Roles of the Neutrophil in Sepsis: Protective and Deleterious.
696 *Front. Immunol.* **7**, 155 (2016).
- 697 28. Spiller, F. *et al.* Hydrogen Sulfide Improves Neutrophil Migration and Survival in Sepsis via
698 K ATPChannel Activation. *Am. J. Respir. Crit. Care Med.* **182**, 360–368 (2010).
- 699 29. Spiller, F. *et al.* 1-Acid Glycoprotein Decreases Neutrophil Migration and Increases
700 Susceptibility to Sepsis in Diabetic Mice. *Diabetes* **61**, 1584–1591 (2012).
- 701 30. Vimr, E. R. & Troy, F. A. Identification of an inducible catabolic system for sialic acids (nan)
702 in *Escherichia coli*. *J. Bacteriol.* **164**, 845–853 (1985).
- 703 31. Butler, C. C. *et al.* Oseltamivir plus usual care versus usual care for influenza-like illness in
704 primary care: an open-label, pragmatic, randomised controlled trial. *Lancet* **395**, 42–52
705 (2020).
- 706 32. Rittirsch, D., Huber-Lang, M. S., Flierl, M. A. & Ward, P. A. Immunodesign of experimental
707 sepsis by cecal ligation and puncture. *Nat. Protoc.* **4**, 31–36 (2009).
- 708 33. Rhodes, A. *et al.* Surviving Sepsis Campaign: International Guidelines for Management of
709 Sepsis and Septic Shock: 2016. *Crit. Care Med.* **45**, 486–552 (2017).
- 710 34. Chou, E. H. *et al.* Incidence, trends, and outcomes of infection sites among hospitalizations
711 of sepsis: A nationwide study. *PLoS One* **15**, e0227752 (2020).

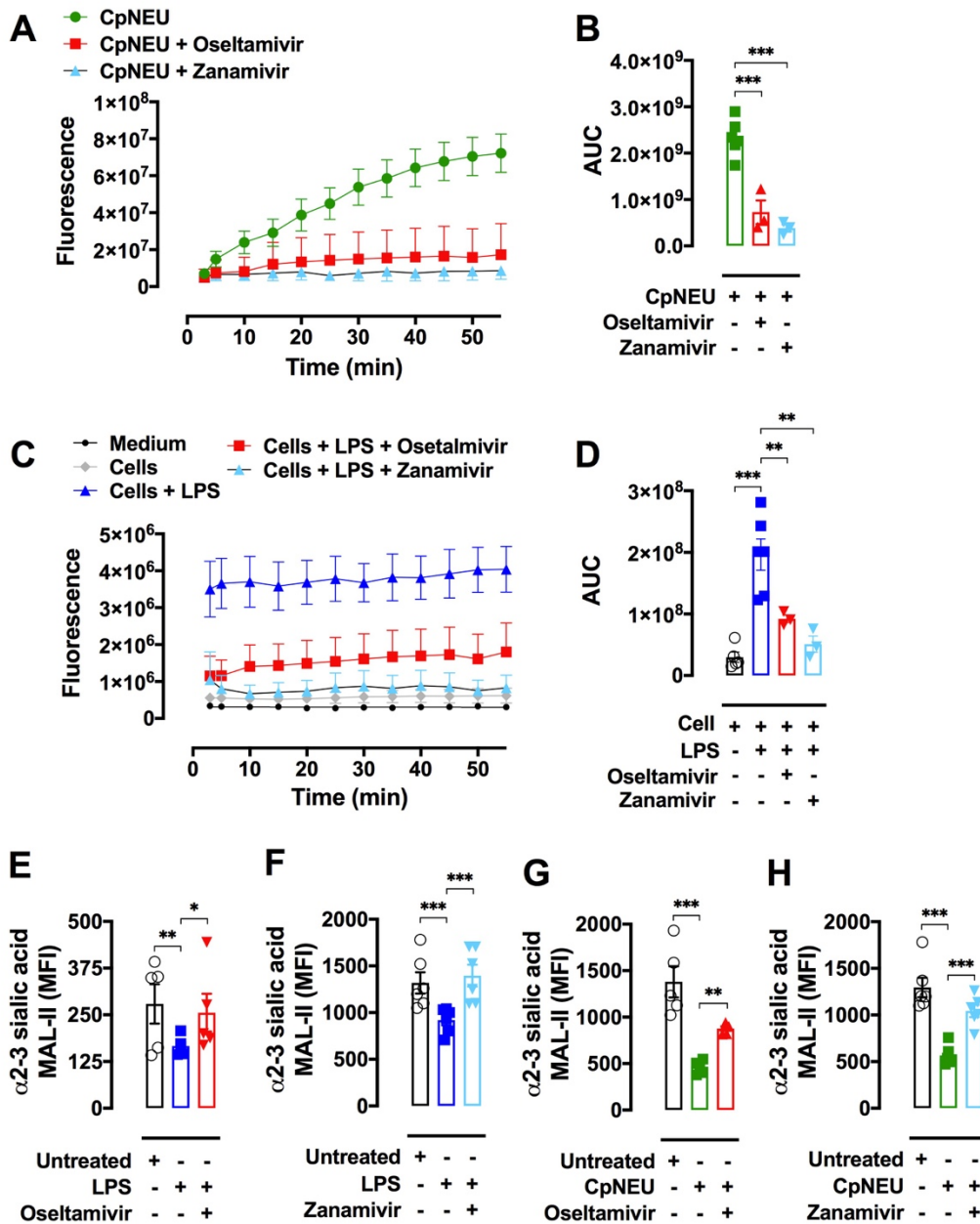
- 712 35. Middleton, E. A. *et al.* Neutrophil extracellular traps contribute to immunothrombosis in
713 COVID-19 acute respiratory distress syndrome. *Blood* **136**, 1169–1179 (2020).
- 714 36. Schurink, B. *et al.* Viral presence and immunopathology in patients with lethal COVID-19: a
715 prospective autopsy cohort study. *Lancet Microbe*. **7**, e290-e299 (2020).
- 716 37. Huang, C. *et al.* Clinical features of patients infected with 2019 novel coronavirus in Wuhan,
717 China. *Lancet* **395**, 497–506 (2020).
- 718 38. Guan, W.-J. *et al.* Clinical Characteristics of Coronavirus Disease 2019 in China. *N. Engl. J.*
719 *Med.* **382**, 1708–1720 (2020).
- 720 39. Silvin, A. *et al.* Elevated Calprotectin and Abnormal Myeloid Cell Subsets Discriminate
721 Severe from Mild COVID-19. *Cell* **182**, 1401–1418.e18 (2020).
- 722 40. Wilk, A. J. *et al.* A single-cell atlas of the peripheral immune response in patients with
723 severe COVID-19. *Nat. Med.* **26**, 1070–1076 (2020).
- 724 41. Kuri-Cervantes, L. *et al.* Comprehensive mapping of immune perturbations associated with
725 severe COVID-19. *Sci Immunol* **5**, (2020).
- 726 42. Schulte-Schrepping, J. *et al.* Severe COVID-19 Is Marked by a Dysregulated Myeloid Cell
727 Compartment. *Cell* **182**, 1419–1440.e23 (2020).
- 728 43. Leliefeld, P. H. C., Wessels, C. M., Leenen, L. P. H., Koenderman, L. & Pillay, J. The role of
729 neutrophils in immune dysfunction during severe inflammation. *Crit. Care* **20**, 73 (2016).
- 730 44. Smutova, V. *et al.* Structural basis for substrate specificity of mammalian neuraminidases.
731 *PLoS One* **9**, e106320 (2014).
- 732 45. Glanz, V. Y., Myasoedova, V. A., Grechko, A. V. & Orekhov, A. N. Sialidase activity in
733 human pathologies. *Eur. J. Pharmacol.* **842**, 345–350 (2019).
- 734 46. Cross, A. S. *et al.* Recruitment of murine neutrophils in vivo through endogenous sialidase
735 activity. *J. Biol. Chem.* **278**, 4112–4120 (2003).
- 736 47. Pshezhetsky, A. V. & Hinek, A. Where catabolism meets signalling: neuraminidase 1 as a
737 modulator of cell receptors. *Glycoconj. J.* **28**, 441–452 (2011).

- 738 48. Abdulkhalek, S. *et al.* Neu1 sialidase and matrix metalloproteinase-9 cross-talk is essential
739 for Toll-like receptor activation and cellular signaling. *J. Biol. Chem.* **286**, 36532–36549
740 (2011).
- 741 49. Feng, C. *et al.* Sialyl residues modulate LPS-mediated signaling through the Toll-like
742 receptor 4 complex. *PLoS One* **7**, e32359 (2012).
- 743 50. Blander, J. M. & Medzhitov, R. Regulation of phagosome maturation by signals from toll-
744 like receptors. *Science* **304**, 1014–1018 (2004).
- 745 51. Doyle, S. E. *et al.* Toll-like receptors induce a phagocytic gene program through p38. *J.*
746 *Exp. Med.* **199**, 81–90 (2004).
- 747 52. El-Benna, J., Dang, P. M.-C. & Gougerot-Pocidallo, M.-A. Priming of the neutrophil NADPH
748 oxidase activation: role of p47phox phosphorylation and NOX2 mobilization to the plasma
749 membrane. *Semin. Immunopathol.* **30**, 279–289 (2008).
- 750 53. Brinkmann, V. Neutrophil Extracellular Traps Kill Bacteria. *Science* **303**, 1532–1535 (2004).
- 751 54. Böhmer, R. H., Trinkle, L. S. & Staneck, J. L. Dose effects of LPS on neutrophils- in a
752 whole blood flow cytometric assay of phagocytosis and oxidative burst. *Cytometry* **13**, 525–
753 531 (1992).
- 754 55. Rifat, S. *et al.* Expression of sialyltransferase activity on intact human neutrophils. *J.*
755 *Leukoc. Biol.* **84**, 1075–1081 (2008).
- 756 56. Cross, A. S. *et al.* Recruitment of Murine Neutrophils in Vivo through Endogenous Sialidase
757 Activity. *J. Biol. Chem.* **278**, 4112–4120 (2003).
- 758 57. Feng, C. *et al.* Endogenous PMN sialidase activity exposes activation epitope on
759 CD11b/CD18 which enhances its binding interaction with ICAM-1. *J. Leukoc. Biol.* **90**, 313–
760 321 (2011).
- 761 58. Sakarya, S. *et al.* Mobilization of neutrophil sialidase activity desialylates the pulmonary
762 vascular endothelial surface and increases resting neutrophil adhesion to and migration
763 across the endothelium. *Glycobiology* **14**, 481–494 (2004).

- 764 59. Petri, B., Phillipson, M. & Kubes, P. The Physiology of Leukocyte Recruitment: An In Vivo
765 Perspective. *J. Immunol.* **180**, 6439–6446 (2008).
- 766 60. Worthen, G., Schwab, B., Elson, E. & Downey, G. Mechanics of stimulated neutrophils: cell
767 stiffening induces retention in capillaries. *Science* **245**, 183–186 (1989).
- 768 61. Sheu, C.-C. *et al.* Clinical characteristics and outcomes of sepsis-related vs non-sepsis-
769 related ARDS. *Chest* **138**, 559–567 (2010).
- 770 62. Wang, T. *et al.* Comorbidities and multi-organ injuries in the treatment of COVID-19. *Lancet*
771 **395**, e52 (2020).
- 772 63. Wu, Z. & McGoogan, J. M. Characteristics of and Important Lessons From the Coronavirus
773 Disease 2019 (COVID-19) Outbreak in China: Summary of a Report of 72 314 Cases From
774 the Chinese Center for Disease Control and Prevention. *JAMA* **323**, 1239–1242 (2020).
- 775 64. Hottz, E. D. *et al.* Platelet activation and platelet-monocyte aggregate formation trigger
776 tissue factor expression in patients with severe COVID-19. *Blood* **136**, 1330–1341 (2020).
- 777 65. Wang, J., Jiang, M., Chen, X. & Montaner, L. J. Cytokine storm and leukocyte changes in
778 mild versus severe SARS- CoV- 2 infection: Review of 3939 COVID- 19 patients in China
779 and emerging pathogenesis and therapy concepts. *J. Leukoc. Biol.* **108**, 17–41 (2020).
- 780 66. Vogl, T. *et al.* Autoinhibitory regulation of S100A8/S100A9 alarmin activity locally restricts
781 sterile inflammation. *J. Clin. Invest.* **128**, 1852–1866 (2018).
- 782 67. Liu, J. *et al.* Clinical outcomes of COVID-19 in Wuhan, China: a large cohort study. *Ann.*
783 *Intensive Care* **10**, 99 (2020).
- 784 68. Czaikoski, P. G. *et al.* Neutrophil Extracellular Traps Induce Organ Damage during
785 Experimental and Clinical Sepsis. *PLoS One* **11**, e0148142 (2016).
- 786 69. Mestriner, F. L. A. C. *et al.* Acute-phase protein alpha-1-acid glycoprotein mediates
787 neutrophil migration failure in sepsis by a nitric oxide-dependent mechanism. *Proc. Natl.*
788 *Acad. Sci. U. S. A.* **104**, 19595–19600 (2007).
- 789 70. National Research Council, Division on Earth and Life Studies, Institute for Laboratory

- 790 Animal Research & Committee for the Update of the Guide for the Care and Use of
791 Laboratory Animals. *Guide for the Care and Use of Laboratory Animals: Eighth Edition*.
792 (National Academies Press, 2011).
- 793 71. Kilkenny, C., Browne, W. J., Cuthill, I. C., Emerson, M. & Altman, D. G. Improving
794 bioscience research reporting: the ARRIVE guidelines for reporting animal research. *PLoS*
795 *Biol.* **8**, e1000412 (2010).
- 796 72. Xu, J. *et al.* A fixation method for the optimisation of western blotting. *Sci. Rep.* **9**, 6649
797 (2019).
- 798

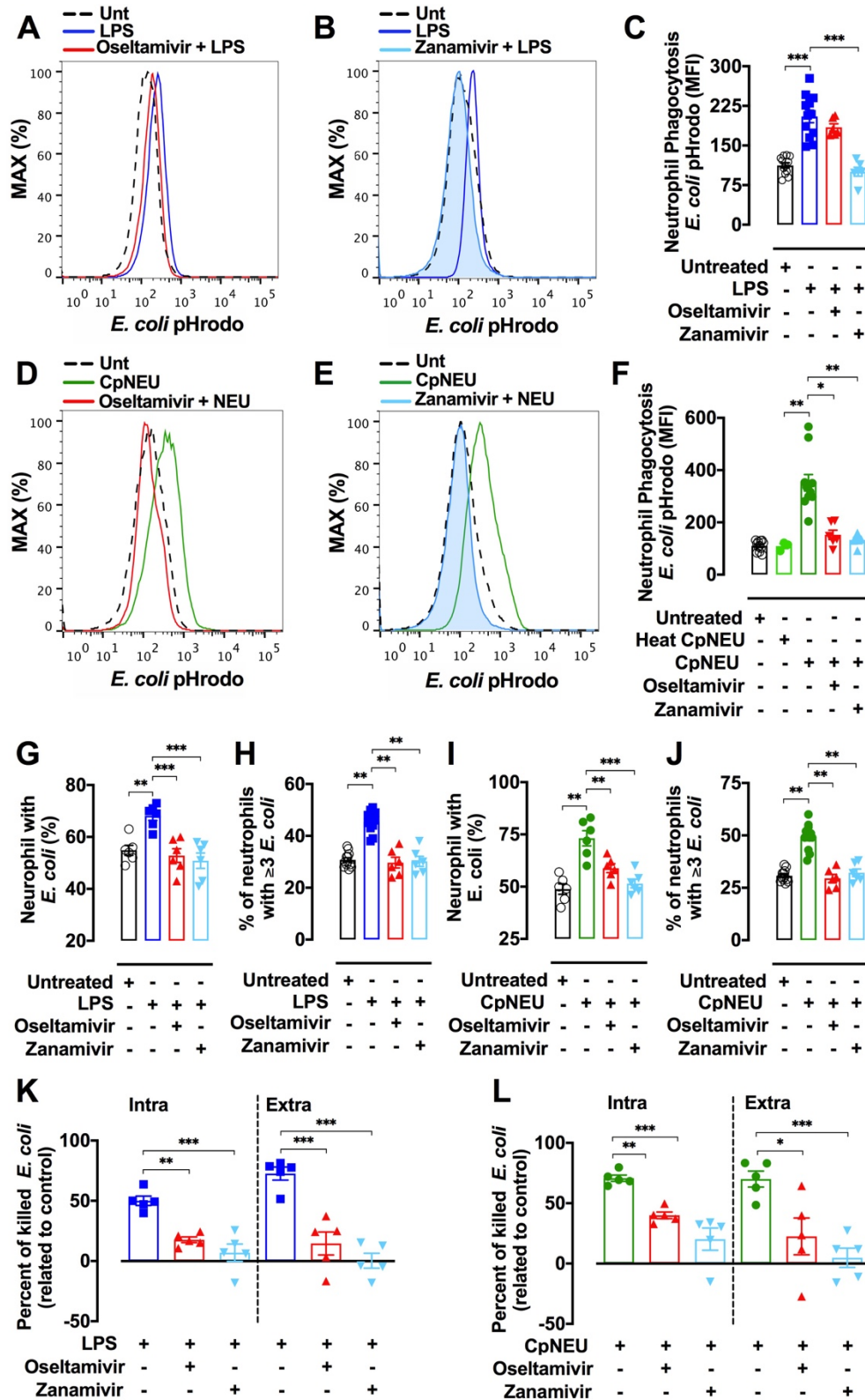
799 **Figures and Figure Legends**
800



801
802

803 **Figure 1. LPS stimulates NEU activity in human leukocytes.** Neuraminidase isolated
804 from *Clostridium perfringens* (CpNEU) was used to validate the NEU activity assay.
805 CpNEU (0.012 UI) was added in a 96-well flat-bottom dark plate on ice in the presence
806 or not of its inhibitors Oseltamivir phosphate (100 μM) or Zanamivir (30 μM). Next, the
807 substrate 4-MU-NANA (0.025 mM) was added and the fluorescent substrate was read 3
808 min after at 37 °C (A). The area under the curve (AUC) values are shown in B. Total

809 leukocytes resuspended in HBSS were added in a plate on ice and 4-MU-NANA
810 substrate (0.025 mM) was added followed by the addition of medium, LPS (1 µg/mL),
811 LPS plus Oseltamivir (100 µM) or LPS plus Zanamivir (30 µM). The fluorescent
812 substrate was read 3 min after at 37 °C (**C**). Raw data were subtracted from the control
813 group containing only HBSS (medium) and expressed as AUC values (**D**). Whole blood
814 containing 1×10^6 leukocytes from healthy donors were stimulated or not with LPS (1
815 µg/mL, 90 min, 37 °C, 5% CO₂), LPS plus Oseltamivir (100 µM), or LPS plus Zanamivir
816 (30 µM). Total leukocytes (1×10^6) were incubated with CpNEU (10 mU, 60 min, 37 °C,
817 5% CO₂), CpNEU plus Oseltamivir (100 µM), or CpNEU plus Zanamivir (30 µM).
818 Leukocytes were stained with MAL-II to detect α2-3 sialic acids (**E-F**). The MFI was
819 analyzed on CD66b⁺ cells using the gate strategies shown in Supplementary Fig. 1. **P*
820 < 0.05; ***P* < 0.01; ****P* < 0.001. This figure is representative of three independent
821 experiments (n= 3-6) and data are shown as mean ± SEM. LPS = lipopolysaccharide;
822 MAL-II = *Maackia amurensis* lectin II; CpNEU = neuraminidase.
823



824

825

826

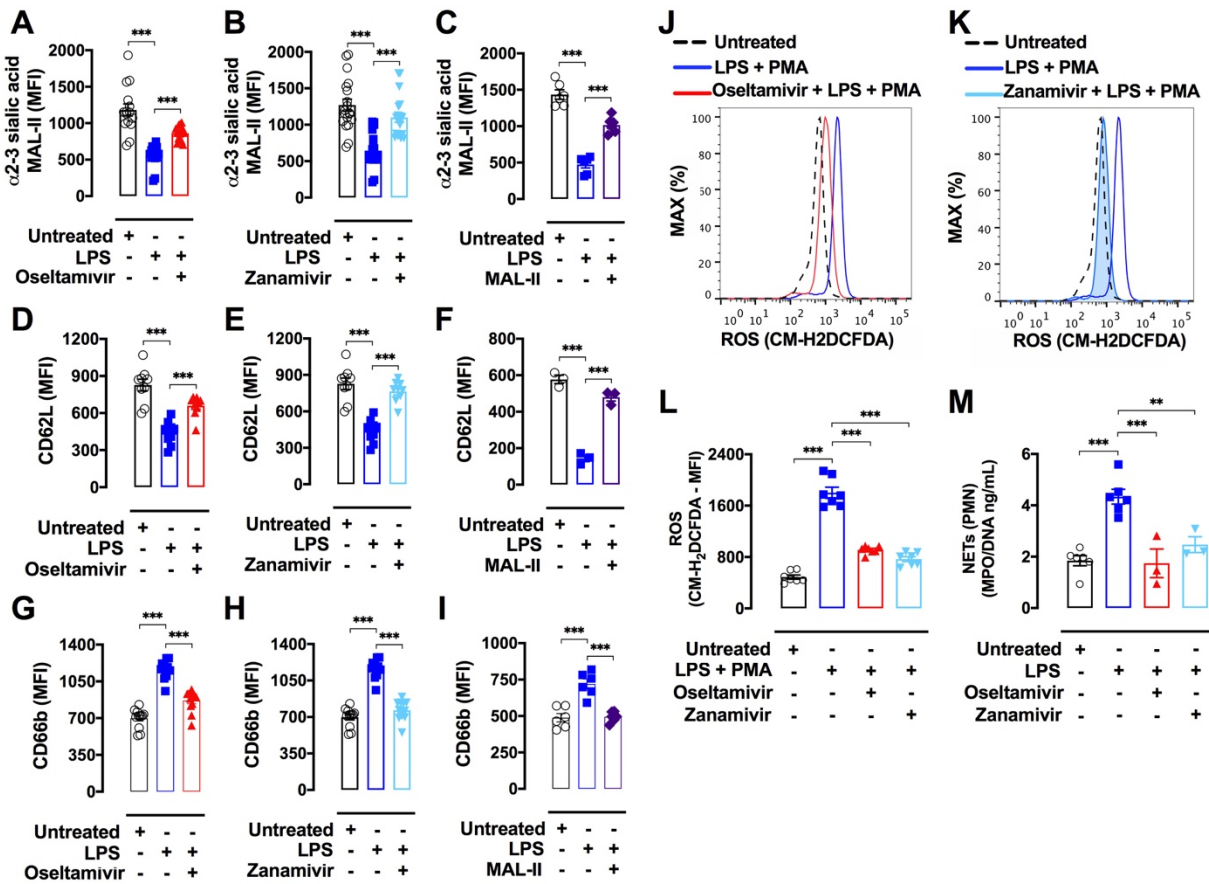
Figure 2. LPS increases phagocytosis and killing of *E. coli* in a NEU-dependent

manner. Whole blood from healthy donors containing 1×10^6 leukocytes were exposed

827 (37 °C, 5% CO₂) or not to LPS (1 µg/mL, 90 min), LPS plus Oseltamivir (100 µM), or
828 LPS plus Zanamivir (30 µM) (**A-C; G-H; K**). Total leukocytes (1 x 10⁶) were exposed or
829 not to CpNEU (10 mU, 60 min, 37 °C, 5% CO₂), CpNEU plus Oseltamivir (100 µM), or
830 CpNEU plus Zanamivir (30 µM) (**D-F; I-J; L**) and the phagocytosis and killing assays
831 were performed. Leukocytes were incubated with *E. coli* pHrodo BioParticles® (100
832 µg/mL) for 60 min at 37 °C to assess phagocytosis in viable CD66b⁺ cells (**A-F**) (as
833 gated in Supplementary Fig. 1). Live *E. coli* was used to evaluate phagocytosis by light
834 microscopy or to assess the killing by leukocytes. Cells were stimulated as described
835 above and 1 x10⁶ leukocytes were incubated at 37 °C with *E. coli* (1 x10⁶ CFU) for 90
836 min for phagocytosis or for 180 min for killing assays. The percentage of cells with
837 ingested bacteria (**G; I**) and the number of bacterial particles per cell (**H; J**, ≥3 particles
838 per cell) were evaluated. The killing of *E. coli* was evaluated by spreading 10 µL of
839 supernatant (extracellular killing) or 10 µL of the intracellular content in agar medium
840 and the CFU were counted. Killing *E. coli* was expressed as the rate of fold change
841 compared to the unprimed (untreated) cells (**L**). Symbols represent individual donors
842 and data are shown as mean ± SEM from pooled data of two to three independent
843 experiments (n = 3-12). **P* < 0.05; ***P* < 0.01; ****P* < 0.001. Unt = untreated; LPS =
844 lipopolysaccharide; CpNEU = neuraminidase.

845
846

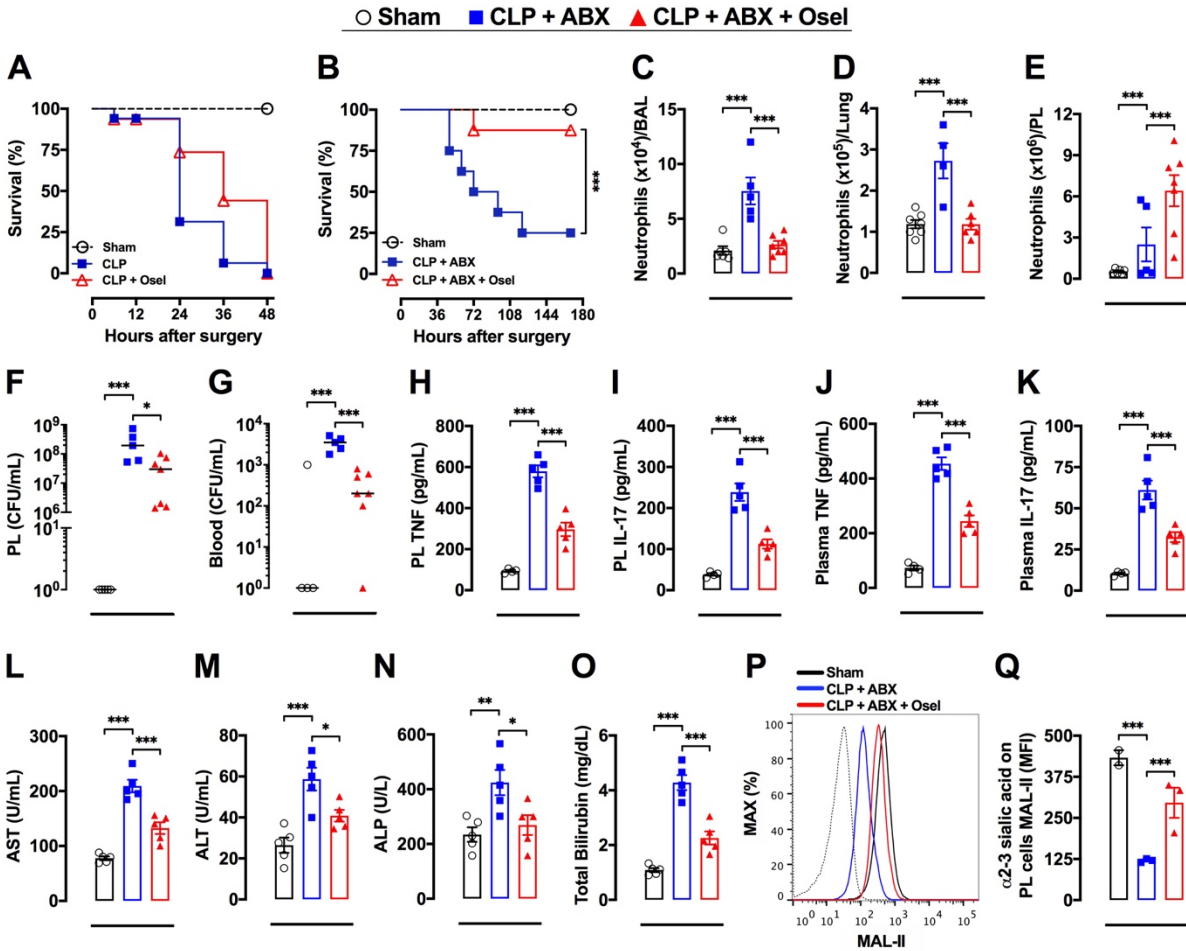
847



848
849

850 **Figure 3. LPS-induced human neutrophil response involves NEU activity.** Whole
851 blood from healthy donors containing 1×10^6 leukocytes were stimulated or not with
852 LPS ($1 \mu\text{g/mL}$, 90 min, 37°C , 5% CO_2), LPS plus Osetamivir ($100 \mu\text{M}$), LPS plus
853 Zanamivir ($30 \mu\text{M}$), or LPS plus MAL-II ($1 \mu\text{g/mL}$, MAL-II promotes steric hindrance at
854 the NEU cleavage site and prevent sialic acid cleavage). Leukocytes were marked with
855 MAL-II to detect α 2-3 sialic acids (**A-C**) or stained with the cell activation markers
856 CD62L (**D-F**) and CD66b (**G-I**). After RBCs lysis leukocytes were incubated with $5 \mu\text{M}$
857 CM-H2DCFDA fluorescent probe for 15 min. PMA ($10 \mu\text{M}$) was used to stimulate ROS
858 production for 10 min (**J-L**). Supplementary Fig. 5 showed ROS production in additional
859 control groups. The MFI was analyzed on CD66b^+ cells using the gate strategies shown
860 in Supplementary Fig. 1. Isolated neutrophils were treated with Osetamivir ($100 \mu\text{M}$) or
861 Zanamivir ($30 \mu\text{M}$) 1 h before the stimulus with LPS ($10 \mu\text{g/mL}$) for 4 h. The
862 concentration of NETs was evaluated by MPO-DNA PicoGreen assay on supernatants

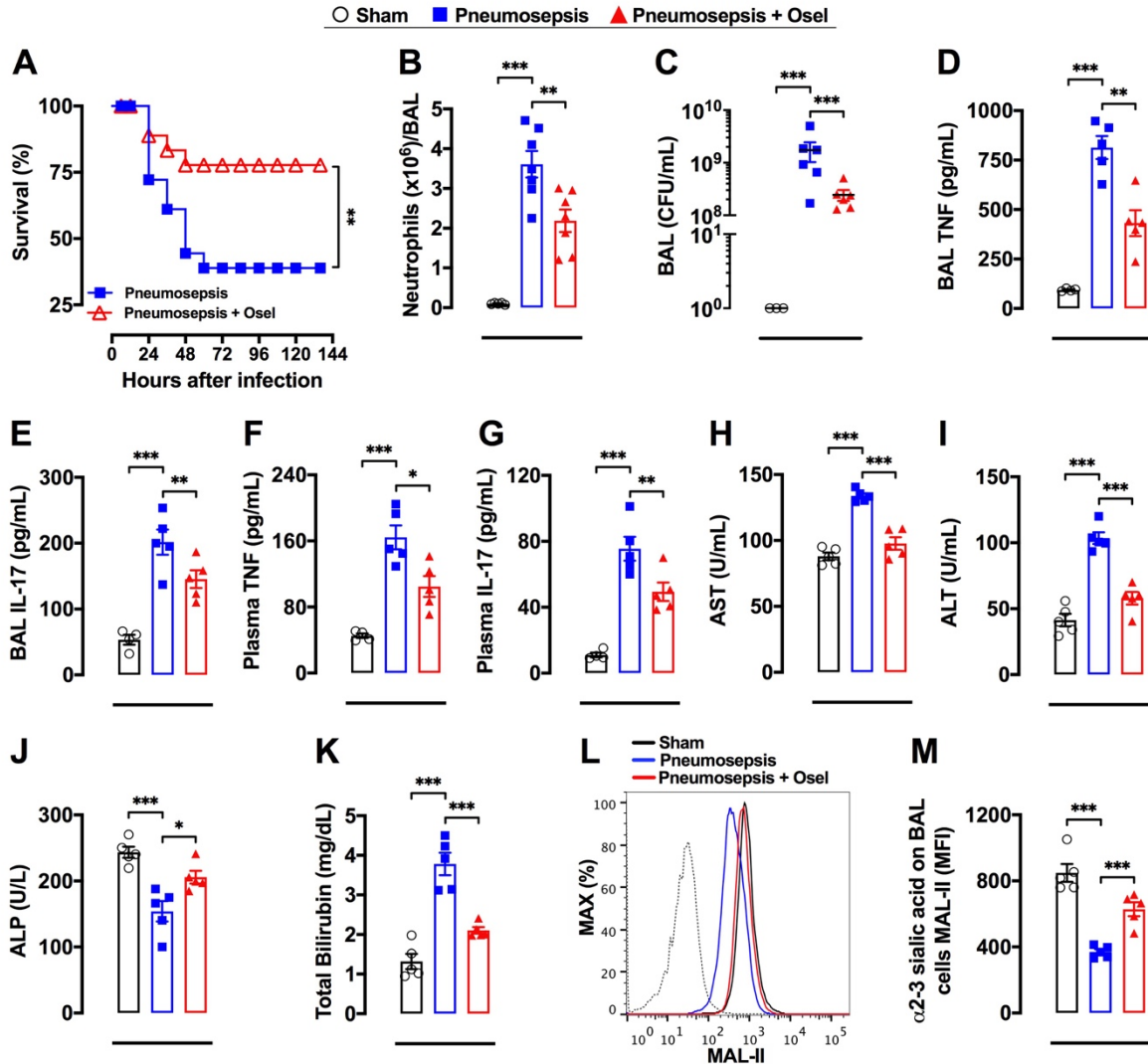
863 of cells (**M**). Symbols represent individual donors and data are shown as mean \pm SEM
864 from pooled data of two to three independent experiments ($n = 7$) except for F and M
865 that was made once with $n=3$. *** $P < 0.001$; ** $P < 0.01$. Unt = untreated; CM-H2DCFDA
866 = 5-(and-6)-chloromethyl-2',7'-dichlorodihydrofluorescein diacetate, acetyl ester; LPS =
867 lipopolysaccharide; PMA = phorbol 12-myristate 13-acetate; ROS = reactive oxygen
868 species; NETs = neutrophil extracellular traps; RBCs = red blood cells; MAL-II =
869 *Maackia amurensis* lectin II; PMN = polymorphonuclear leukocytes.



870
871

872 **Figure 4. Osetamivir enhanced host survival in CLP-induced sepsis.** Severe
873 sepsis was induced by the cecal ligation and puncture (CLP) model. Mice were
874 randomly treated (starting 6 hr after infection, 12/12 h, PO, for 36 hr, n=16) with saline
875 or Osetamivir phosphate (10 mg/kg) and their survival rates were monitored over 48 hr
876 (A). In another set of experiments, CLP mice were randomly IP treated (started 6 hr
877 after infection, 12/12 hr) during 4 days with 100 μ L metronidazole (15
878 mg/kg)/ceftriaxone (40 mg/kg) (ABX) plus saline or Osetamivir phosphate (10 mg/kg)
879 by PO and their survival rates (n=12) were monitored over 168 hr (B). Also, mice were
880 subjected to CLP and treated with ABX + saline or ABX + Osetamivir as described in B
881 and euthanized 48 hr after surgery to evaluate the number of neutrophils in BAL (C),
882 lung tissue (D), and peritoneal lavage (PL) (E); TNF (H), IL-17 (I), and CFU (F) were
883 also determined in PL. Blood CFU (G) and plasmatic levels of TNF (J), IL-17 (K), AST
884 (L), ALT (M), ALP (N) and total bilirubin (O) were also evaluated 48 hr after surgery.

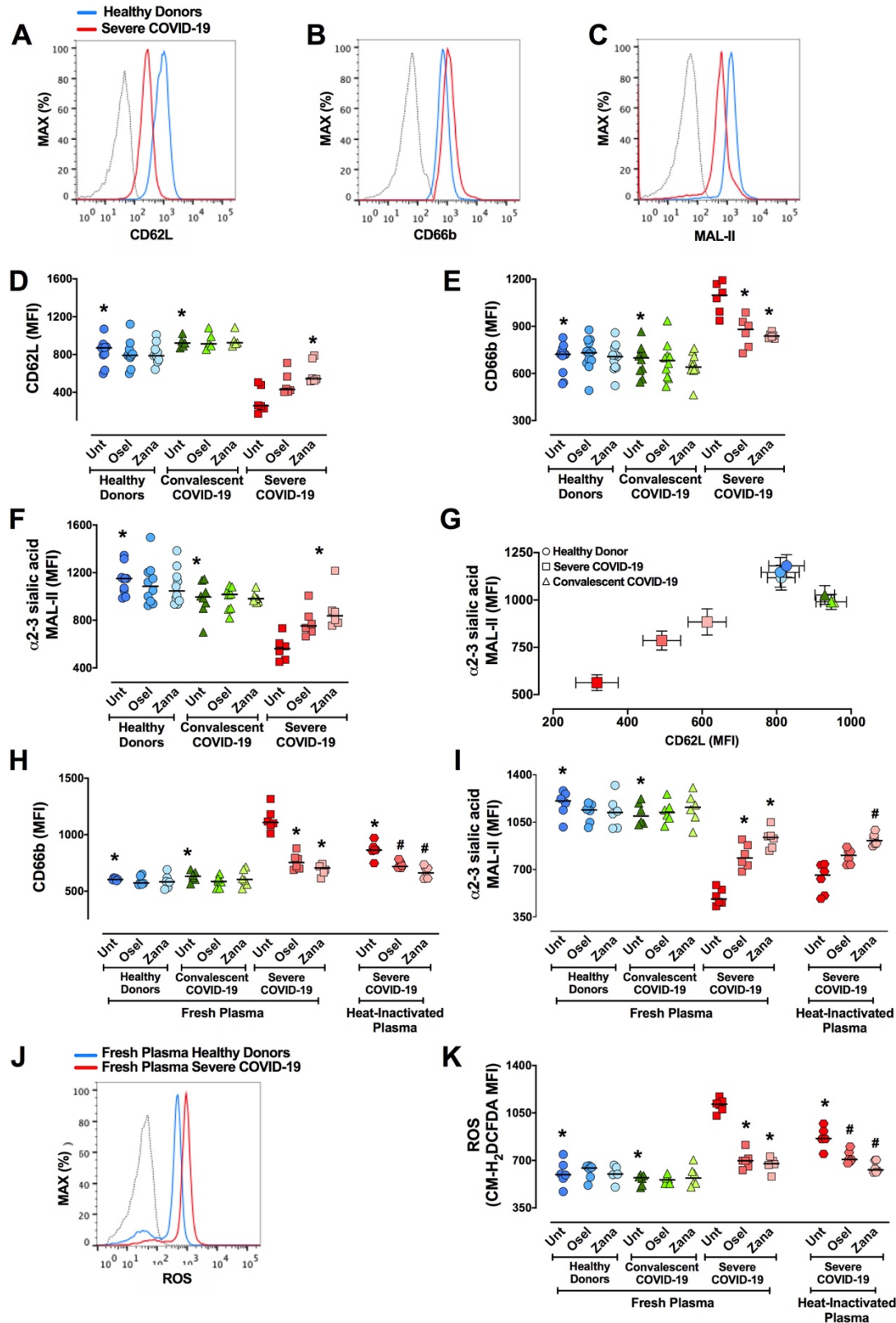
885 The amount of surface α 2-3 sialic acids were assessed by MAL-II staining in
886 SSC^{high}/Gr-1^{high} cells in PL and analyzed by FACS, as shown by the representative
887 histograms (**P**) and MFI (**Q**); dotted line = unstained cells. The results are expressed as
888 percent of survival (n=16), mean or median (only for FACS data) \pm SEM. **P* < 0.05; ****P*
889 < 0.001. These experiments were repeated 3 times for survival analysis and twice for
890 other parameters (n=3-7). ABX = antibiotics (metronidazole/ceftriaxone); Sham = sham-
891 operated. Osel = Oseltamivir; AST = alanine aminotransferase; ALT = aspartate
892 aminotransferase; ALP = alkaline phosphatase; CFU = colony-forming units.



893 **Figure 5. Osetamivir enhanced mice survival in *K. pneumoniae*-induced sepsis.**

894 Sepsis was induced by intratracheal administration of *K. pneumoniae* and mice were
 895 randomly treated (starting 6 hr after infection, 12/12 hr, PO, n=20) with saline or
 896 Osetamivir phosphate (10 mg/kg) and survival rates were monitored for 144 hr (A). In
 897 similar set of experiments, septic mice (n=6-7) were treated 6 hr after infection with a
 898 single dose of Osetamivir phosphate (10 mg/kg, PO) and mice were euthanized 24 hr
 899 after infection to determine the number of neutrophils (B) and CFUs (C), and levels of
 900 TNF (D) and IL-17 (E) in BAL. Plasma levels of TNF (F), IL-17 (G), AST (H), ALT (I),
 901 ALP (J) and total bilirubin (K) were also evaluated 24 hr after infection. The amount of
 902 surface α2-3 sialic acids were assessed by MAL-II staining in SSC^{high}/Gr-1^{high} cells in
 903 BAL and analyzed by FACS, as shown by the representative histograms (L) and MFI
 904

905 **(M)**; dotted line = unstained cells. The results are expressed as percent of survival,
906 mean or median (only for FACS data) \pm SEM. * P < 0.05; * P < 0.01; *** P < 0.001. Sham
907 = sham-operated mice; Osel = Oseltamivir; AST = alanine aminotransferase; ALT =
908 aspartate aminotransferase; ALP = alkaline phosphatase.



909
910
911

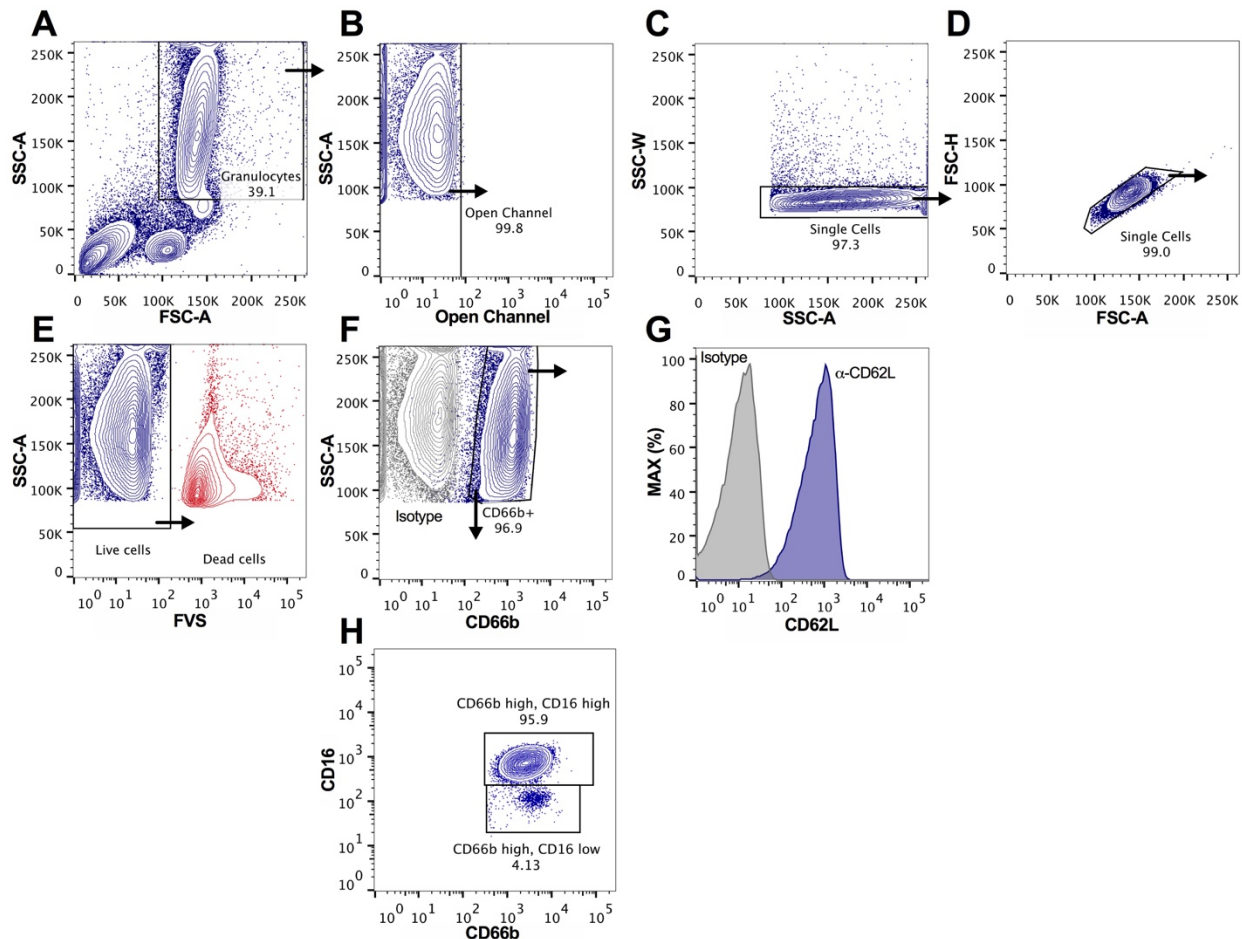
Figure 6. Osetamivir and Zanamivir decrease neutrophil activation and increase α 2-3 sialic acid levels in active, but not convalescent neutrophils from COVID-19

912 **patients.** Whole blood from healthy donors (n= 10), severe COVID-19 patients (n= 6) and
913 convalescent COVID-19 patients (n= 8) were treated or not with Oseltamivir (100 μ M) or
914 Zanamivir (30 μ M) and total leukocytes were stained with the cell activation markers
915 CD62L (**A and D**), CD66b (**B and E**) and MAL-II to detect α 2-3 sialic acids (**C and F**).
916 Correlation of surface levels of α 2-3 sialic acids vs CD62L (**G**). Blood samples from
917 healthy donors (n = 7) were incubated for 2 h (37 °C, 5% CO₂) with 7% of fresh plasma
918 from healthy donors, severe or convalescent COVID-19 patients or with 7% of heat-
919 inactivated plasma from severe COVID-19 patients in the presence or absence of
920 Oseltamivir (100 μ M) or Zanamivir (30 μ M) and levels of CD66b (**H**), surface α 2-3-Sia
921 (MAL-II) (**I**), and ROS production (**J, K**) were assessed by FACS. The MFI was analyzed
922 on CD66b⁺ cells using the gate strategies shown in Supplementary Fig. 1. Symbols
923 represent individual donors and data are shown as scatter dot plot with line at median
924 from pooled data of two to seven independent experiments. The statistical significance
925 between the groups was assessed by ANOVA followed by a multiple comparisons test of
926 Tukey. The accepted level of significance for the test was P<0.05. * was significantly
927 different when compared with Untreated Severe COVID-19; # was significantly different
928 when compared with Untreated Heat-Inactivated Plasma from Severe COVID-19. Osel =
929 Oseltamivir; Zana = Zanamivir.
930

931 **Supplementary Data**

932 **Supplementary Figures and Figure Legends**

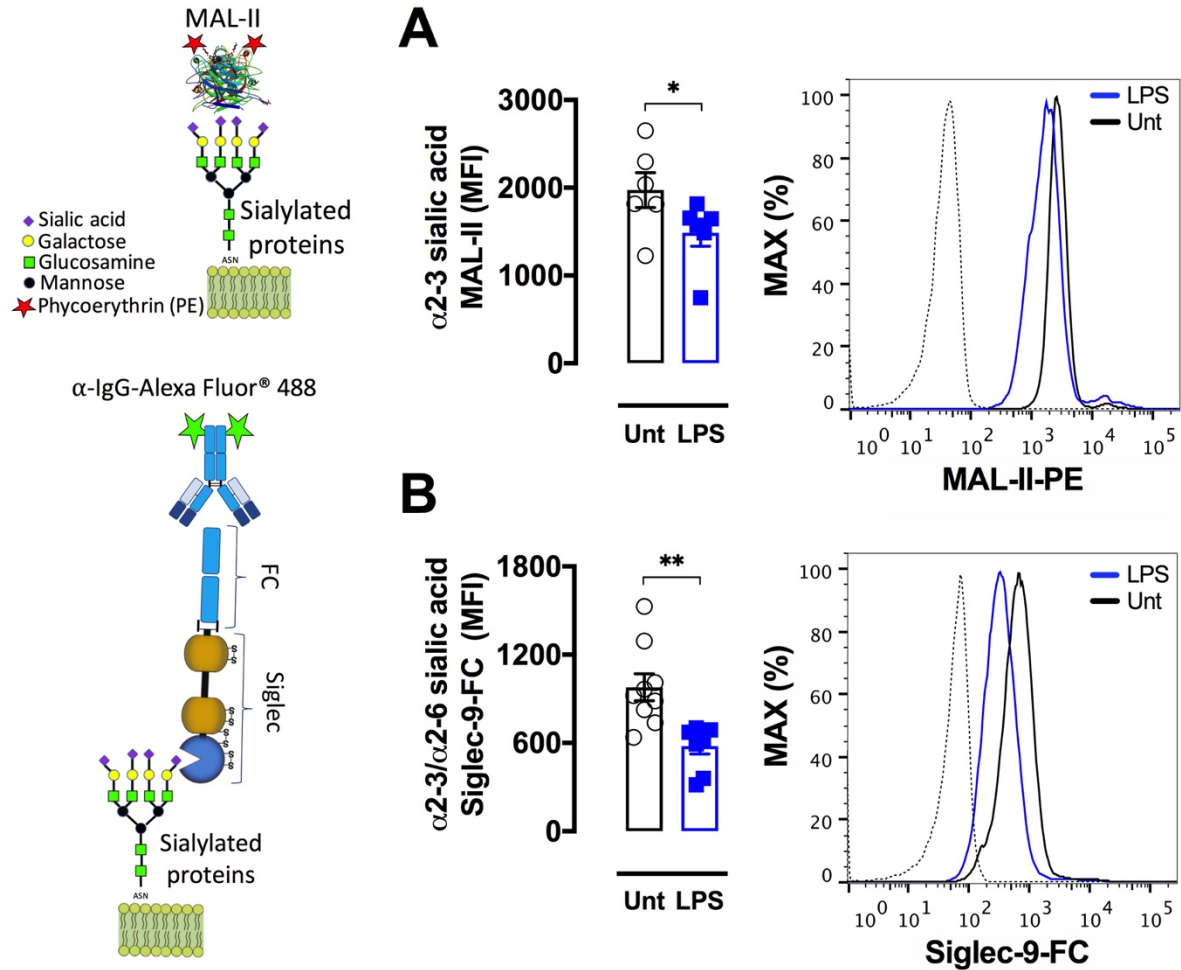
933



934

935 **Supplementary Fig. 1. Representative gate strategy used for neutrophils analysis.**

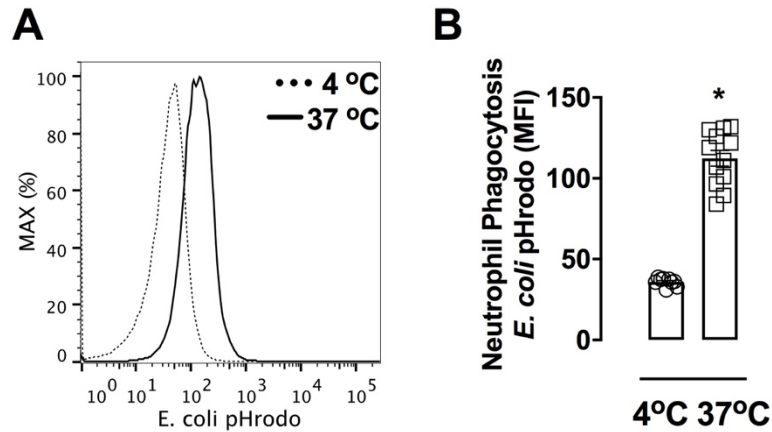
936 A classic forward-scatter (FSC) vs side-scatter (SSC) characteristic dot plot was used to
937 select neutrophils population (A) from peripheral blood collected from healthy donors
938 and patients. Autofluorescent (B) and doublets (C-D) were excluded and live cells were
939 selected (E). CD66b⁺ positive cells (F) were gated and the MFI of surface markers, such
940 as CD62L (G) were assessed. Around 96% of CD66b⁺ cells are mature neutrophils
941 (CD66b-high/CD16-high) and 4% of CD66b⁺ cells are CD66b-high/CD16-low, which is
942 suggestive of immature neutrophils or eosinophils (H). Approximately 100.000 gated
943 events were collected in each analysis. The analysis was performed in a FACSVerse
944 using FACSsuite software (BD Biosciences) and FlowJo software (FlowJo LLC).



945

946 **Supplementary Fig. 2. LPS reduces surface $\alpha 2-3$ sialic acids from human**
 947 **neutrophils.** Whole blood containing 1×10^6 leukocytes from healthy donors were
 948 stimulated with $1 \mu\text{g}/\text{mL}$ LPS for 90 min and $\alpha 2-3$ sialic acid contents were assessed by
 949 staining cells with biotinylated *Maackia Amurensis* Lectin II (MAL-II) (A) followed by
 950 streptavidin-phycoerythrin (PE) incubation. Siglec-9 ligands (B) were labeled by
 951 incubation of chimeric protein containing Siglec-9 sialic acid-Ig binding domain fused to
 952 a human IgG-Fc portion (Siglec-9-Fc). Siglec-Fc-9 were incubated with α -IgG1-Alexa
 953 Fluor 488 before adding the probe to cells. The MFI was analyzed on $\text{CD}66\text{b}^+$ cells
 954 using the gate strategies shown in [Supplementary Fig. 1](#). * $P < 0.05$. Symbols represent
 955 individual donors and data are shown as mean \pm SEM from pooled data of two to three
 956 independent experiments ($n=6-9$). Unt = untreated cells; LPS = lipopolysaccharide;
 957 dotted line = unstained cells.

958



959
960

961 **Supplementary Fig. 3. Phagocytosis of *E. coli* pHrodo bioparticles at 4 °C and 37**

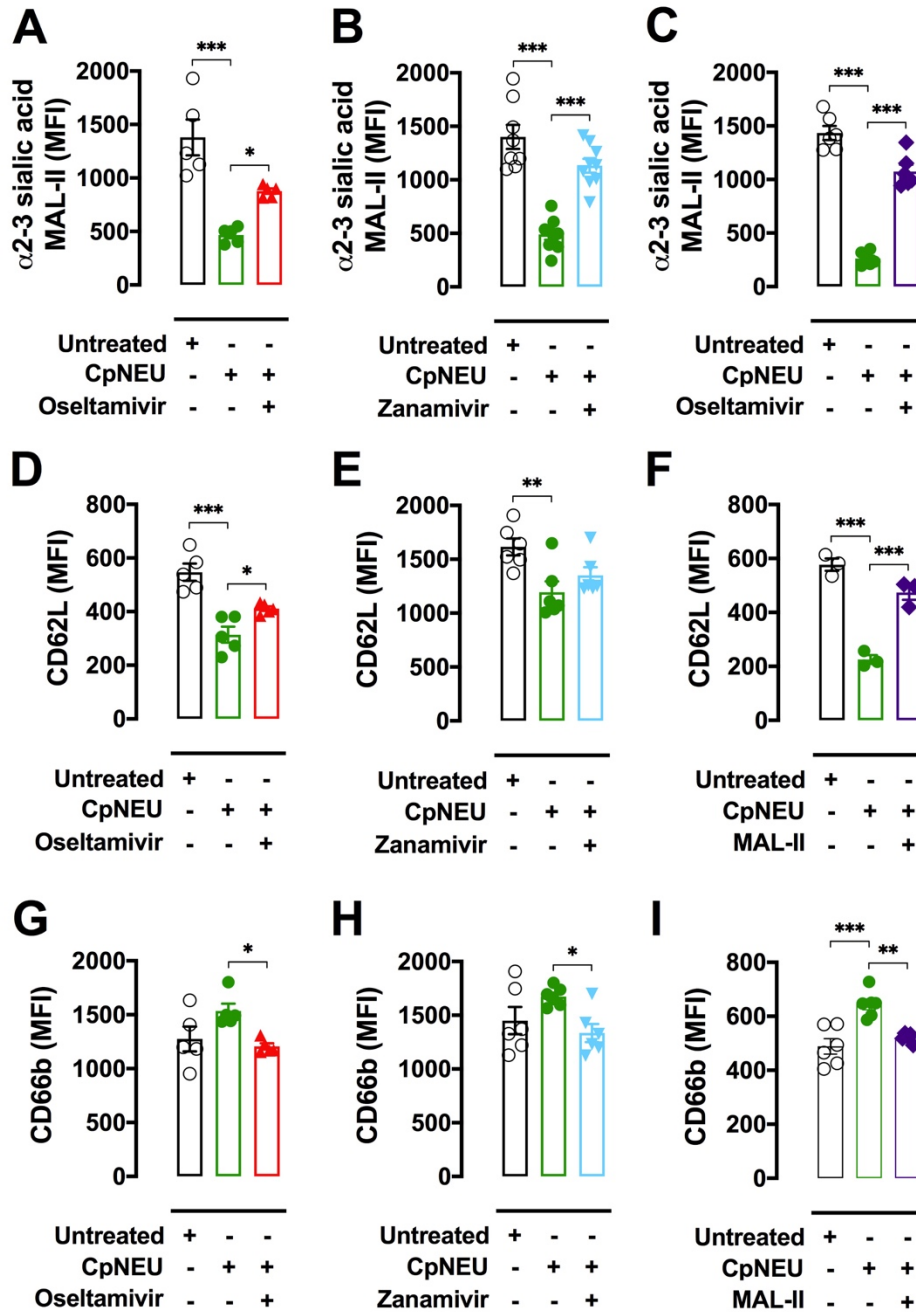
962 °C. Total leukocytes (1×10^6) were incubated with *E. coli* pHrodo bioparticles (100

963 $\mu\text{g}/\text{mL}$) for 60 min at 4 °C or 37 °C and the phagocytosis in viable CD66b⁺ cells was

964 assessed. Symbols represent individual donors and data are shown as mean \pm SEM

965 from pooled data of three to four independent experiments (n = 9-12). * $P < 0.001$.

966



967

968

969

970

971

972

973

Supplementary Fig. 4. CpNeu-induced human neutrophil activation. Total

leukocytes (1×10^6) were incubated or not with CpNEU (10 mU, 60 min, 37 °C, 5%

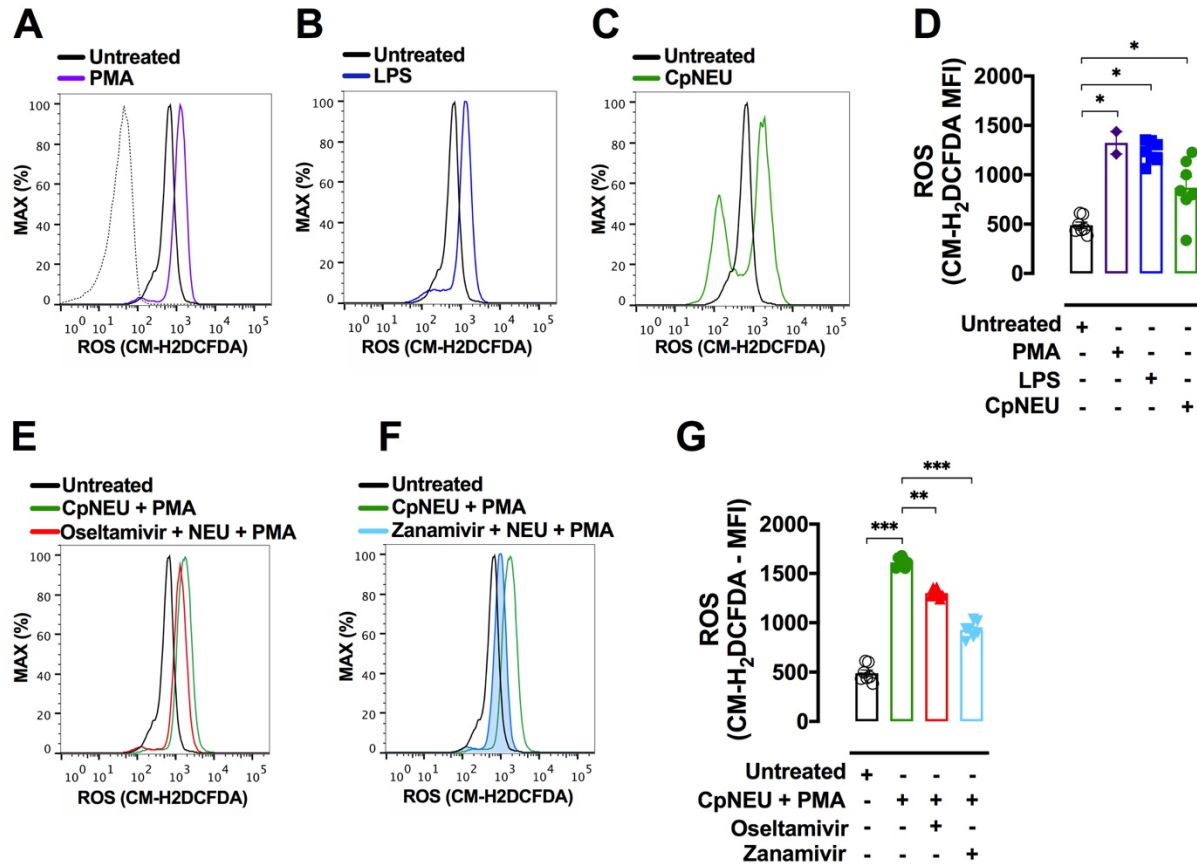
CO₂) CpNEU plus Osetamivir (100 μM), CpNEU plus Zanamivir (30 μM) or CpNEU plus

MAL-II (1 μg/mL). Leukocytes were stained with MAL-II to detect $\alpha 2-3$ sialic acids (A-C)

or with cell activation markers CD62L (D-F) and CD66b (G-I). The MFI was analyzed on

CD66b⁺ cells. Symbols represent individual donors and data are shown as mean \pm SEM

974 from pooled data of two to three independent experiments (n = 5-9) except for F that
975 was made once with n=3. * $P < 0.05$; ** $P < 0.01$; *** $P < 0.001$. MAL-II = *Maackia*
976 *amurensis* lectin II; CpNEU = neuraminidase *Clostridium perfringens*.
977

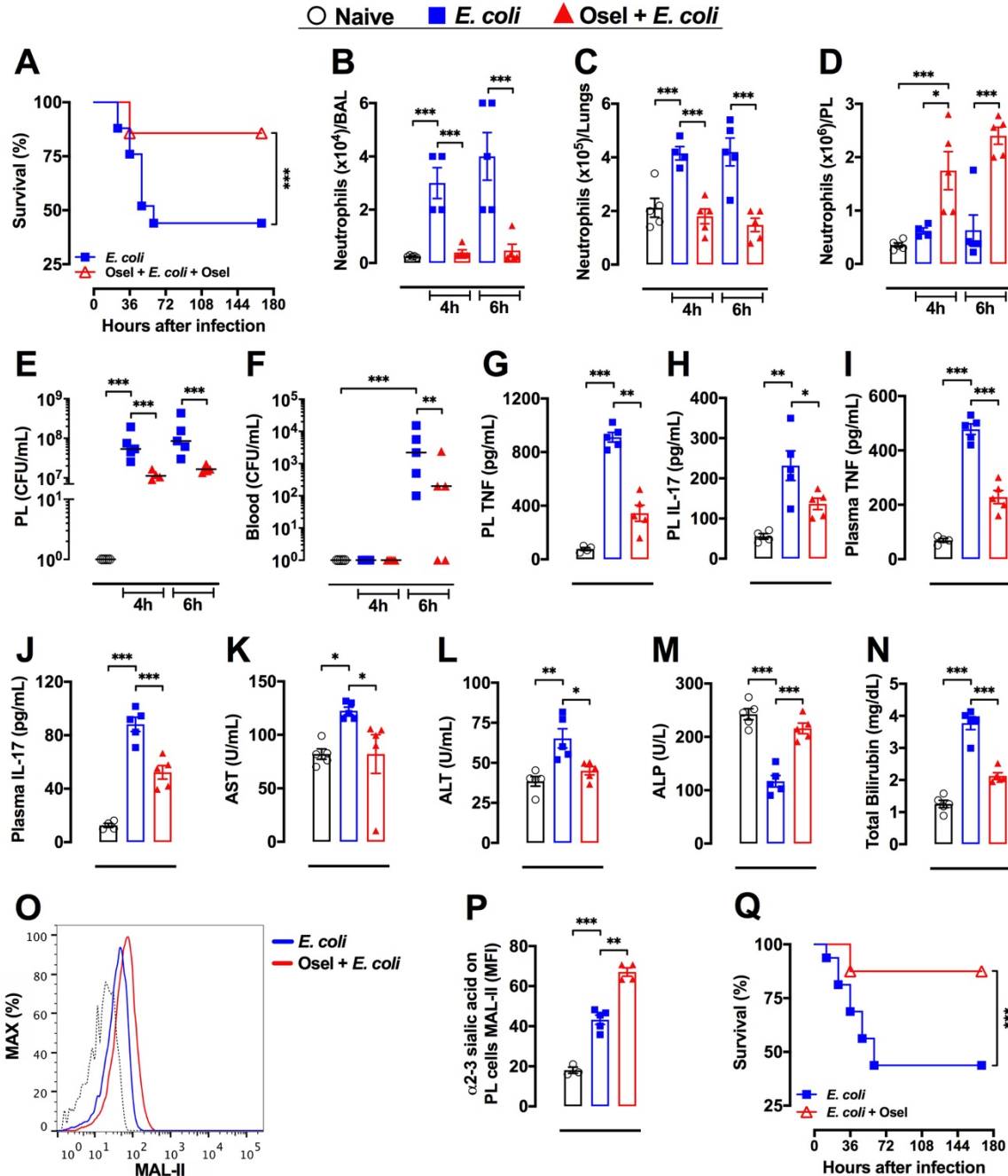


978

979 **Supplementary Fig. 5. ROS production in neutrophils stimulated with LPS,**

980 **CpNEU, or PMA.** Whole blood from healthy donors containing 1×10^6 leukocytes were
 981 exposed or not to LPS ($1 \mu\text{g/mL}$, 90 min) (**B and D**). Total leukocytes (1×10^6) were
 982 incubated or not with CpNEU (10 mU, 60 min) (**C-D**), CpNEU plus Oseltamivir ($100 \mu\text{M}$)
 983 or CpNEU plus Zanamivir ($30 \mu\text{M}$) (**E-G**). Leukocytes were incubated with $5 \mu\text{M}$ CM-
 984 H2DCFDA fluorescent probe for 15 min and PMA ($10 \mu\text{M}$) was used to stimulate ROS
 985 production for 10 min (**A and E-G**). The MFI was analyzed on CD66b^+ cells. Symbols
 986 represent individual donors and data are shown as mean \pm SEM from pooled data of
 987 two independent experiments ($n = 2-6$). $*P < 0.05$; $**P < 0.01$; $***P < 0.001$. C = control;
 988 CM-H2DCFDA = 5-(and-6)-chloromethyl-2',7'-dichlorodihydrofluorescein diacetate,
 989 acetyl ester; LPS = lipopolysaccharide; CpNEU = neuraminidase *Clostridium*
 990 *perfringens*; PMA = phorbol 12-myristate 13-acetate.

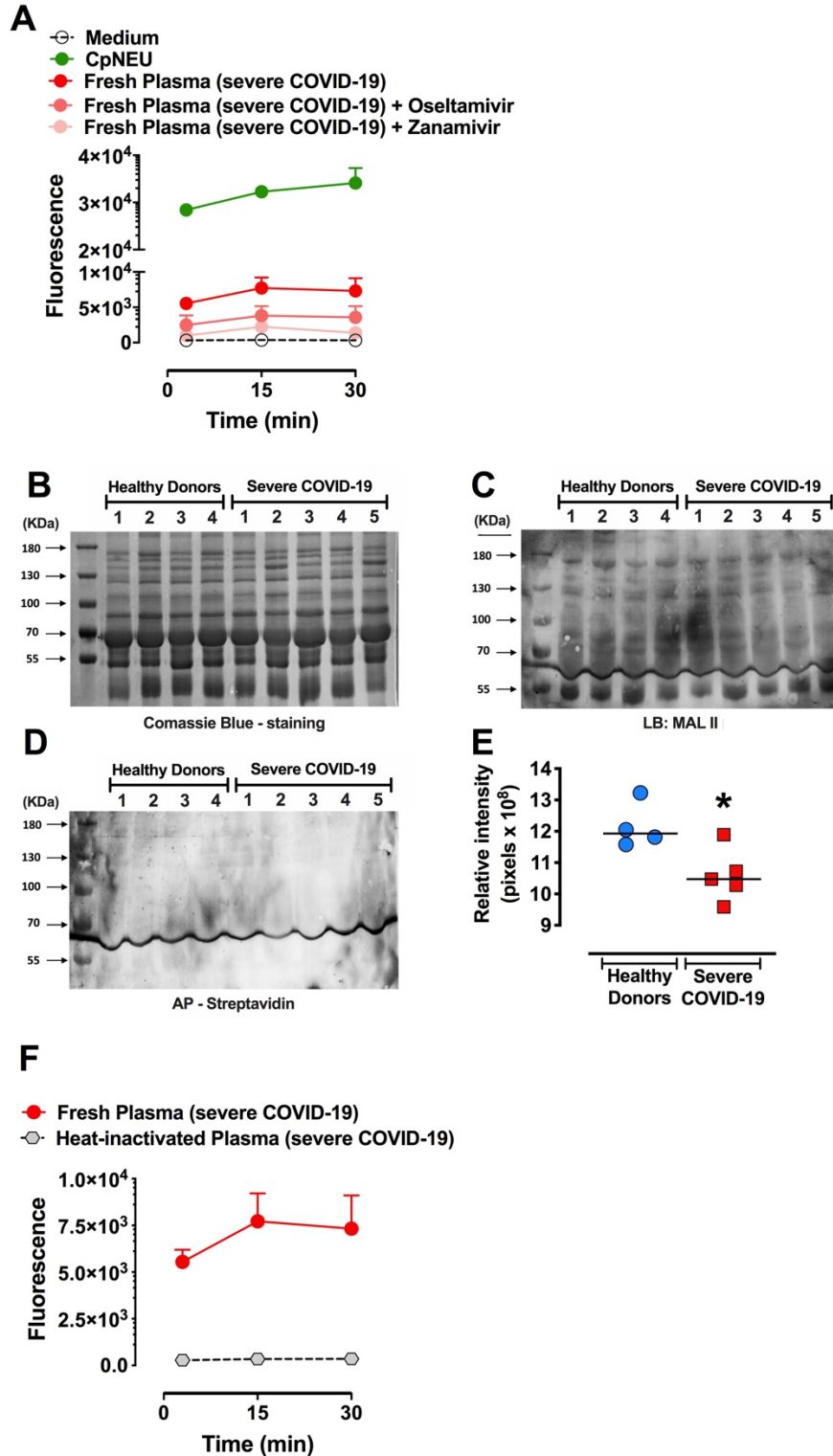
991



992

993 **Supplementary Fig. 6. Osetamivir improved the outcome of *E. coli*-induced**
 994 **sepsis.** Sepsis was induced by intraperitoneal (IP) administration of 1×10^7 CFU/mice
 995 *E. coli* (ATCC 25922). Mice were randomly pretreated *per oral* (PO) via (2 hr before
 996 infection) and posttreated (6 hr after infection, 12/12 hr, PO, for 4 days) with Osetamivir
 997 phosphate (Osel, 10 mg/Kg) or saline and their survival rates were monitored over 168
 998 hr (A, n=16). In another set of experiments (n=3-5) mice were randomly pretreated (2 hr

999 before infection) with Oseltamivir phosphate (10 mg/Kg, PO) and the number of
1000 neutrophils in bronchoalveolar lavage (BAL, **B**) and in lung tissue (**C**) was counted. In
1001 peritoneal lavage (PL) infiltrating neutrophils counts (**D**), TNF (**G**), IL-17 (**H**) and the
1002 number of colony-forming units (CFU) in PL (**E**) or blood (**F**) were determined 4 or 6 hr
1003 after infection. Plasma levels of TNF (**I**), IL-17 (**J**), AST (**K**), ALT (**L**), ALP (**M**) and total
1004 bilirubin (**N**) were evaluated. The amount of surface α 2-3 sialic acids were also
1005 assessed in PL SSC^{high}/Gr-1^{high} cells as shown by the representative histograms (**O**) or
1006 MFI (**P**); dotted line = unstained cells. Mice were also randomly posttreated (starting 6
1007 hr after infection, 12/12 hr, PO, for 4 days) with saline or Oseltamivir phosphate (10
1008 mg/Kg) and their survival rates were monitored over 168 hr (**Q**). The results are
1009 expressed as percent of survival (n=16), mean or median (only for FACS data) \pm SEM.
1010 * P < 0.05; ** P < 0.01; *** P < 0.001. These experiments were repeated 3 times for
1011 survival analysis and twice for other parameters. Osel = Oseltamivir; AST = alanine
1012 aminotransferase; ALT = aspartate aminotransferase; ALP = alkaline phosphatase;
1013 MAL-II = *Maackia amurensis* lectin II.



1014

1015

Supplementary Fig. 7. NEU activity is increased in plasma from severe COVID-19

1016

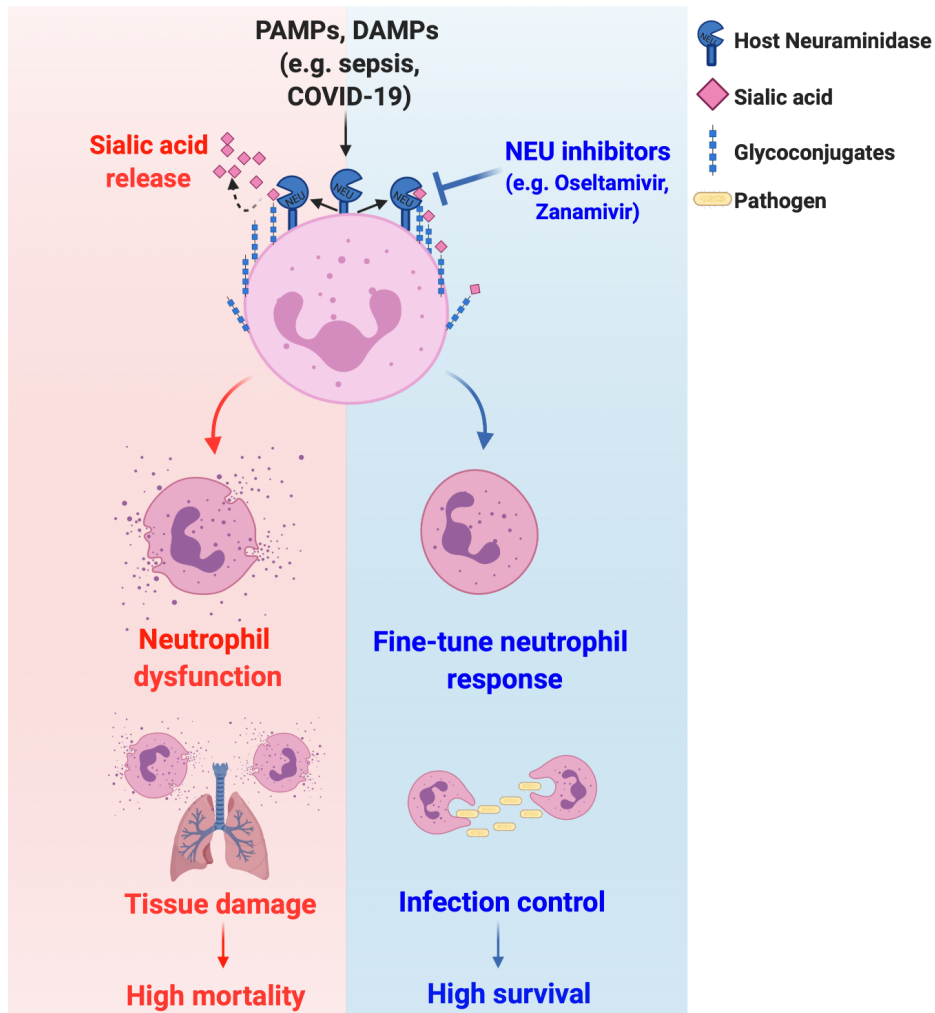
patients. NEU activity was evaluated in fresh plasma from severe COVID-19 patients in

1017

the presence or absence of Oseltamivir (100 μ M) or Zanamivir (30 μ M) (A) and in heat-

1018 inactivated plasma from COVID-19 patients **(F)**. Neuraminidase isolated from
1019 *Clostridium perfringens* (CpNEU) was used to validate the NEU activity assay. Twelve
1020 µg of total serum proteins from healthy donors (n=4) or severe COVID-19 patients (n=5)
1021 were separated by SDS-PAGE 10% and stained with coomassie blue **(B)**. Lectin
1022 blotting (LB) were performed with biotin-conjugated MAL-II for staining α2-3 sialic acid-
1023 containing proteins **(C)** or membrane were incubated with AP-Streptavidin without MAL-
1024 II (as a control) **(D)**. The intensity of lectin staining of each lane was evaluated and
1025 normalized to the total proteins on corresponding gel lanes **(E)**; *p=0.02 Unpaired t test -
1026 Welch's correction. MAL-II = *Maackia amurensis* lectin II; CpNEU = neuraminidase
1027 *Clostridium perfringens*.
1028
1029

1030



1031

1032

1033

1034

1035

1036

1037

1038

1039

Supplementary Fig. 8. Working model. PAMPs and DAMPs in severe diseases such as sepsis and COVID-19 lead to neuraminidase activation with shedding of surface sialic acid and neutrophil overactivation, resulting in tissue damage and high mortality rates. On the other hand, neuraminidase inhibitors (e.g., Oseltamivir, Zanamivir) prevent the sialic acid release to regulates neutrophil response, resulting in infection control and high survival rates.

1040 **Supplementary Table 1.**

1041

1042 **Supplementary Table 1. Clinical information of samples from UFSC University**

1043 **Hospital, SC, Brazil**

1044

	Severe COVID-19	Convalescent COVID-19
Characteristic		
Gender (Male/Female)	3/2	7/5
Age (years)	44.4 (25;65)	53.2 (36;80)
Weight (kilos)	90.0 (62.2;127)	85.1 (51.8;150)
Height (m)	1.72 (1.65;1.8)	1.7 (1.55;1.83)
Cough	4 (80%)	8 (66.7%)
Dyspnea	4 (80%)	5 (41.7%)
Chest Pain / Oppression	1 (20%)	4 (33.3%)
Asthenia	2 (40%)	3 (16.7%)
Myalgia	3 (60%)	3 (16.7%)
Anosmia	1 (20%)	5 (41.7%)
Ageusia / Dysgeusia	1 (20%)	4 (33.3%)
Fever	3 (60%)	3 (16.7%)

Paresthesia	0 (0%)	0 (0%)
Headache	0 (0%)	2 (16.7%)
Diarrhea	0 (0%)	1 (8.3%)
Diabetes mellitus	3 (60%)	4 (33.3%)
Systolic BP (mmHg)	132.2 (100;150)	126.4 (100;177)
Diastolic BP (mmHg)	84.2 (80;90)	78.55 (60;102)
Heart rate (bpm)	96.4 (80;115)	86.4 (72;115)
Respiratory frequency (bpm)	20.8 (18;25)	20.8 (11;29)
Length of hospitalization (days)	6.6 (4;10)	8.3 (3;16)
Mechanical ventilation	0 (0%)	3 (16.7%)
Mechanical ventilation time (days)	0 (0%)	7.3 (5;9)
Saturation (O2%)	90.4 (85;97)	93.3 (86;99)
SOFA Score	0.17 (0;1)	0.6 (0;2)

Laboratory data

Hemoglobin (g/dL)	13.5 (11;15)	13.65 (11.3;15.7)
Hematocrit (%)	40 (33.4;47.1)	40.2 (34.8;45.5)

Leukocytes (/μL)	7988 (4070;12930)	8098 (5330;10660)
Neutrophils (/μL)	5731 (3355;10098)	6448.5 (3923;9135)
Lymphocytes (/μL)	1526 (451;3728)	955.8 (208;1687)
Monocytes (/μL)	369 (253;483)	473.2 (168;961)
Platelets (x10 ³ /μL)	235 (115;314)	238 (117;436)
PCR (mg / dL)	52.5 (22;78.7)	90.7 (15;214)

1045
1046
1047

1048 **Supplementary Table 2. Clinical information of**
1049 **samples from Hospital Naval Marcílio Dias, RJ,**
1050 **Brazil**

	Severe COVID-19
<hr/>	
<i>Characteristic</i>	
<hr/>	
Gender (Male/Female)	2/3
Age (years)	66 (55-73)
Cough	4 (80%)
Dyspnea	4 (80%)
Chest Pain / Oppression	0 (0%)
Asthenia	1 (20%)
Myalgia	2 (40%)
Anosmia	2 (40%)
Ageusia / Dysgeusia	0 (0%)
Fever	4 (80%)
Paresthesia	0 (0%)
Headache	0 (0%)
Diarrhea	3 (60%)

Diabetes mellitus	3 (60%)
Systolic BP (mmHg)	141.4 (108;166)
Diastolic BP (mmHg)	74.8 (51;100)
Heart rate (bpm)	83.8 (57;102)
Respiratory frequency (bpm)	24 (14-40)
Length of hospitalization (days)	32.8 (10;90)
Mechanical ventilation	5 (100%)
Saturation (O ₂ %)	87.3 (83;91)

Laboratory data

Hemoglobin (g/dL)	11.92 (7.9;13.3)
Hematocrit (%)	35.72 (23;41.6)
Leukocytes (/μL)	7900 (5400;12100)
Neutrophils (/μL)	5724.8 (4266;7502)

Lymphocytes (/μL)	983.8 (430;1694)
Monocytes (/μL)	575.8 (216;1452)
Platelets (x10 ³ /μL)	172.8 (109;219)
PCR (mg / dL)	15.8 (5.16;26.8)

1051
1052